PHYSICOCHEMICAL CHARACTERIZATION OF Ni-Al_2O_3 AND La-PROMOTED Ni-Al_2O_3 CATALYST FOR METHANE DRY REFORMING

NORZAINI BIN ABD. RAHIM

DEGREE OF BACHELOR OF CHEMICAL ENGINEERING

UNIVERSITI MALAYSIA PAHANG

PHYSICOCHEMICAL CHARACTERIZATION OF Ni-Al_2O_3 AND La-PROMOTED Ni-Al_2O_3 CATALYST FOR METHANE DRY REFORMING

NORZAINI BIN ABD. RAHIM

A thesis submitted in fulfillment of the
requirements for award of the degree of
Bachelor of Chemical Engineering

Faculty of Chemical & Natural Resources Engineering
Universiti Malaysia Pahang

FEBRUARY 2013

SUPERVISOR'S DECLARATION

"I hereby declare that I have checked this thesis and in my opinion, this thesis is adequate in terms of scope and quality for the award of the degree of Bachelor of Chemical Engineering"

Signature : .....

Name of supervisor : Madam Nur Aminatulmimi Ismail

Position : URP Supervisor

Date : 18 February 2013

Signature : .....

Name of supervisor : Dr. Cheng Chin Kui

Position : URP Co-supervisor

Date : 18 February 2013

STUDENT'S DECLARATION

I declare that thesis entitle *"Physicochemical Characterization of Ni-Al_2O_3 and La-Promoted Ni-Al_2O_3 Catalyst for Methane Dry Reforming"* is the result of my own research except as cited in the references. The thesis has not been accepted for any degree and is not concurrently submitted in candidature of any other degree.

Signature : ……..

Name : Norzaini Bin Abd. Rahim

Date : 18 February 2013

Special dedication to my mum and dad that always inspire, love and stand beside me,

and to my beloved friend.

Thank you for all your love, care and support.

ACKNOWLEDGEMENT

Bismillahirrahmanirrahim and Alhamdulillah. Praise to God for His help and guidance that I finally able to complete this Undergraduate Research Project.

First and foremost I would like to thank my supervisors; Madam Nur Aminatulmimi Ismail and Dr. Cheng Chin Kui for giving me the opportunity to work on this interesting project and also, willingness in overseeing the progress of my works from its initial phases till the completion of it. I do believe that all her advice and comments are for the benefit of producing the best thesis quality.

I am also very thankful to beloved my father, my lovely mother, all my family members and also to all my friends around me for their support and motivation. Without the support from all of them, this thesis will become more difficult to finish. I am grateful to everybody that involves directly or indirectly helping me completing this thesis.

I would like to also take this opportunity to thank all lecturers who involved directly and indirectly in helping me to complete this research. For personnel at

FKKSA technical staffs, thank you very much for your guidance, trust and assistance.

To my friends and course mates, that giving endless helps and support, thank you very much, especially under same supervisor. Thanks to former and present colleagues at Universiti Malaysia Pahang for making an enjoyable working environment and giving me ideas, opinions, and advices. Thank you again.

TABLE OF CONTENTS

LIST OF TABLES

LIST OF FIGURES

LIST OF ABBREVIATIONS

ATR	Autothermal reforming
BET	Brunauer, Emmett and teller isotherm
DR	Dry reforming
DRM	Dry reforming of methane
FTIR	Fourier transform infrared spectroscopy
GTL	Gas to liquids
IUPAC	International union of pure & applied chemistry
POX	Partial oxidation
PROX	Preferential reaction oxidation
SMSI	Strong metal-support interactions
SR	Steam reforming
TCD	Thermal conductivity detector
WGS	Water gas shift
XRD	X-ray diffraction
XRF	X-ray fluorescense

LIST OF SYMBOLS

°	Degree.
α_o	Ratio of number of gas of inelastic collisions resulting in absorption to total number of collisions of gas molecules on the surface.
c_α	Polymeric.
c_β	Filamentous.
c_γ	Graphitic.
C	Constant value, characteristic of the adsorbate.
n	Number of adsorbed molecules desorbing in unit area of the surface.
θ	Fraction of surface of covered by adsorbed molecules.
P	Gas pressure.
P_S	Saturation pressure of adsorbed gas.
S_A	Surface area of solid.
μ	Number of molecules colliding in unit time with a unit area of the surface.
V	Volume of gas adsorbed.
V_m	Volume of adsorbed gas corresponding to monolayer coverage.
$\Delta\widehat{H}_f^\circ$	Heat of formation at 25 ^{0}C and 1 atm

LIST OF APPENDICES

CIRI-CIRI FIZIKOKIMIA Ni-Al_2O_3 DAN La-MODIFIKASI Ni-Al_2O_3 PEMANGKIN UNTUK TINDAKBALAS KIMIA ANTARA METANA-KARBON DIOKSIDA

ABSTRAK

Tindakbalas kimia antara metana (CH_4) dan karbon dioxsida (CO_2) telah dijalankan dengan menggunakan Nikel alumina sebagai pemangkin yang disediakan melalui percampuran antara nikel dan lantanum metal pada sokongan alumina pemangkin. Pemangkin 10%Ni-90% Al_2O_3 telah dimodifikasi dengan menggunakan lantaham metal yang mempunyai 3%. Fizikokimia pemangkin dianalisis dengan menggunakan seperti berikut; XRF, FTIR, BET, dan XRD untuk membandingkan diantara 10%Ni – 90%Al_2O_3 dan 3%La – 10%Ni – 90%Al_2O_3 pemangkin untuk tindakbalas kimia antara metana-karbon diokside kepada hidrogen. Melalui XRF analisis, pemangkin – pemangkin menunjukan logam utama berada dalam pemangkin tersebut dalam keadaan susunan formula yang baik seperti pemangkin yang telah dijalankan. Manakala, FTIR analisis pula mengesahkan kehadiran molekul dan pembentukan kumpulan atom dalam molekul struktur yang sama diantara pemangkin tersebut. XRD Analisis juga mengesahkan kehadiran utama kristal di dalam 10%Ni – 90%Al_2O_3 pemangkin adalah aluminate nikel ($NiAl_2O_4$) yang terbentuk disebabkan oleh tindak balas diantara Al_2O_3 dengan NiO pada suhu pengkalsinan yang lebih tinggi. Sifat-sifat fizikal 10%Ni – 90%Al_2O_3 dan 3%La – 10%Ni – 90%Al_2O_3 pemangkin menunjukkan isoterm "*Type IV*", yang mempunyai pemeluwapan kapilari dalam "*mesoporous*" dengan tenaga penjerapan yang tinggi, manakala histerisis "Type H1" mempunyai geometri liang silinder atau zarah-zarah yang berbentuk bola dengam saiz yang seragam. Analisis BET juga mengesahkan bahawa tiada kesan yang ketara di dalam luas permuakan pemangkin tersebut. Manakala purata "Horvat & Kavazoe" liang atau lubang saiz juga mennjukan tiada perubahan yang ketara yang kita dapat lihat. Berdasarkan analisis tersebut saya dapat membuat kesimpulan bahawa modifikasi pemangkin dengan lanthanum metal adalah salah satu pemangkin yang dapat mengurangkan pembetukan karbon dipermukaan pemangkin semasa proses ini berlaku.

PHYSICOCHEMICAL CHARACTERIZATION OF Ni-Al_2O_3 AND La-PROMOTED Ni-Al_2O_3 CATALYST FOR METHANE DRY REFORMING

ABSTRACT

The CO_2 reforming reaction of CH_4 was conducted by using a Ni-based catalyst were prepared by the wet co-impregnation using nickel and lanthanum on alumina support. Monometallic catalyst of 10wt.%Ni-90wt.%Al_2O_3 was promoted with 3wt.% lanthanum metal. The physicochemical of catalysts were characterized by XRF, FTIR, BET, and XRD respectively, which to compare the catalyst between the calcined catalyst of unpromoted (10wt.%Ni-90wt.%Al_2O_3) with 3La promoted (3wt.%La-10wt.%Ni-87wt.%Al_2O_3) performance for methane conversion to hydrogen. XRF analysis for the main metals presented in the calcined catalyst indicated a good agreement with the intended formula. FTIR analysis confirmed the presence of similar structural unit and formation of identical chemical moieties of the unpromoted and 3La promoted catalysts. XRD analysis confirmed the presence of major crystalline unpromoted catalysts is spinel ($NiAl_2O_4$) because it is formed by the reaction of Al_2O_3 with NiO at the higher calcination temperature of the catalyst. The physical attributes for unpromoted and 3La promoted catalyst showed a *Type IV* isotherm, in an indication typical of capillary condensation in mesoporous with high energy of adsorption and a hysteresis loop of *Type H1* under new classification system revealing cylindrical pore geometry or spheroidal particles with reasonably uniform size. BET analysis confirmed that no discernible effect for lanthanum addition to the unpromoted bimetallic catalyst. Also, the similarity between the distribution of average Horvat & Kavazoe desorption pore size for the unpromoted and 3La promoted. Based on this analysis, I can conclude that the modified catalyst with lanthanum metal is one catalyst that will be reducing the formation of carbon on the surface catalyst during this process.

CHAPTER I

INTRODUCTION

This chapter provide the general ideals on the subject that are going to be study including background of study, problem statement, research objectives, scope of proposed study, expected outcome and significance of proposed study.

1.1 Background of Study

In recent years, a lot of interests have been registered for renewable and environmental friendly energy conversion technology such as fuel cell technology application. The current crisis of depleting crude oil resources with associated environmental difficulties inspires enormous numbers of researchers around the

world to consider alternative routes for fuel production such as synthesis gas (syngas) utilization under a gas to liquids (GTL) process. However, since about 50 - 60% of the cost of this process based on the raw material (i.e. syngas) (Pena et al., 1996; Wilhelm et al., 2001), it is therefore an essential requirement to investigate the options for the production of syngas through hydrocarbons and improve them. Besides that, the low temperature fuel cell also requires continuous supply of hydrogen. Among these options, H_2-supplying reaction is via dry reforming of methane has been recently considered as a potential choice given the revolution in catalyst design and reaction operation technologies.

Methane dry reforming (DRM) is a catalytic reaction between methane and carbon dioxide to produce synthesis gas (a mixture of hydrogen and carbon monoxide). However, the main challenge that has prevented this process from commercial application is high thermodynamic potential of coke formation (Gadalla, & Bower, 1988; Hou et al., 2003; Souza et al., 2004) that deactivates the catalyst. However, the process is now being considered with high potential under the vast developments in catalyst design and reactor operation technologies with the aim to reduce carbon deposition. Based on the dry reforming reaction mechanism, carbonaceous residue mainly comes from the hydrocarbon substrate decomposition with slight contribution from a CO disproportion reaction. As a consequence coke formation on the catalyst surface weakens the activity of reaction resulting in lower conversion.

The catalysts based on the noble metals (Rh, Ru, Ir, Pt and Pb) are reportedly to exhibit better activities compared to transition metals (mainly Ni and Co), but the

high cost and limited availability hampered its industrial appeal (Souza et al., 2004). Hence it is imperative to develop alumina-supported Ni-based catalysts for DRM process due to its relatively high activity particularly at higher reaction temperature and also low cost.

Furthermore, in order to improve the carbon deposition resistance of Ni-based catalysts, various promoters such as alkaline, alkaline earth metal and rare earth are impregnated into Ni-based catalysts. In addition, the modifications to the supported catalysts by promoters in CH_4 reforming with CO_2 are common and have been reported before (Cheng et al., 2001; Xu et al., 2001; Junke et al., 2009; Yang, et al., 2010). It was reported that product ratio, selectivity and catalyst stability may improved from the modifications (Wan et al., 2007). In this study, we investigate the physicochemical characterization of Ni/Al_2O_3 and Ni/Al_2O_3 catalysts promoted with rare earth metal (Lanthanum) for methane dry reforming.

1.2 Problem Statement

In the dry reforming of methane process, one of the factors that influence catalyst activity is attributed to the high potential high thermodynamic potential towards coke formation. Through dry reforming reaction mechanism, carbonaceous residue also easily itself formed from the hydrocarbon substrate decomposition with slight contribution from a CO disproportion reaction.

Carbon formation under process can be classified into three main types, namely: poisoning, sintering and coking. While deactivation by poisoning can be eliminated by pre-treatment of the feedstock (Forzatti & Lietti, 1999; Bartholomew, 2001), particular attention to thermal operation conditions under the various stages of the catalytic reaction system is a useful approach to reduce the impact of deactivation by sintering.

In order to improve the catalytic performance, the right choices of supported catalysts are important to ensure that high activity, selectivity, longer lifetime, and thermal stability are attained. Besides that, there are other factors that could improve catalyst attributes for sintering such as the presence of strong metal-support interactions (SMSI), shape and size of the crystallite, support roughness and pore size, and additives present in the support or the metal.

Ni-based catalyst is the most popular catalyst of choice in industries. However, the deactivation occurs easily due to carbon deposition on the catalyst surface. In particular, the catalyst of choice was Ni-based because Ni metal is widely utilizes among the Group VIII transition metals that are normally preferred for reforming reaction, due to acceptable activity combined with low price and wide availability. Also, alumina (Al_2O_3) was commonly used as the support for nickel catalysts because of its high surface area, low cost and thermal stability. However, bimetallic catalysts generally show better activity selectivity, and deactivation resistance compared to monometallic catalysts in reforming reactions. In addition, to improve Ni/Al_2O_3 catalyst, the addition of a basis promoter such as lanthanum (La-

Ni/Al_20_3) could have excellent anti-coking buoyancy and stability and could enhance the thermal attributes of support.

1.3 Research Objectives

The objectives of this research are to prepare a La-promoted Ni/Al_2O_3 catalyst for dry reforming of methane and to investigate the performance of the modified La-Ni/Al_2O_3 catalyst based on the physicochemical characterization.

1.4 Scopes of Study

In order to achieve the objectives, the following scopes have been indentified:

i. Preparation and modification of catalyst using the wet co impregnation technique.
ii. To study the physicochemical properties of the Ni/Al_2O_3 and modified catalyst.

1.5 Rational and Significance of Research

In today's energy supply system, electricity, gasoline, diesel fuel, and natural gas serve as energy carries. These carriers are made by the conversion of primary

energy sources, such as coal, petroleum, underground methane, and nuclear energy, into an energy form that is easily transported and delivered in a usable form to industrial, commercial, residential, and transportation end-users. This study is significant to developments in fuel cell technologies.

CHAPTER II

LITERATURE REVIEW

This chapter provide the general ideals on the subject that are going to be study including the background and introduction of reforming process, hydrogen production from methane, dry reforming of methane and the catalysts used in this study.

2.1 Introduction

Since the beginning of the industrial revolution in the 18th century, fossil fuels in the form of coal, oil, and natural gas have powered the technology and transportation networks that drive the society. This overdependence on fossil fuels

has threatens the supply of energy and causes enormous strains to the environment (Ahmed & Krumpelt, 2001; Williams, 2002).

Today, natural gas is the preferred sources for production of syngas, a mixture of hydrogen and carbon monoxide, from which purified hydrogen can be obtained. There are several different catalytic processes for producing syngas from natural gas (Armor, 2005). Three catalytic chemical processes are used in the conversion of natural gas, composed of hydrocarbons, under a flow of high purity gaseous hydrogen. These three catalytic chemical processes are used sequentially and are described as follows; natural gas reforming, followed by water-gas shift (WGS), and finally a preferential reaction oxidation of CO (PROX).

There are basically four different types of techniques that can be used to carry out the reforming of hydrocarbon; steam reforming (SR), dry reforming (DR), autothermal reforming (ATR), and partial oxidation (POX). All these types of processes have the same purpose and lead to same final product, which is to convert natural gas, mainly composed of hydrocarbon molecules, into syngas.

2.2 Hydrogen Production from Methane

2.2.1 Steam Reforming

The process of methane steam reforming produces syngas with a ratio H_2/CO equals to 3. In this catalytic process, methane reacts with water steam in the presence

of a catalyst. The product of this reaction is syngas (Rostrup-Nielsen, 1984). The scheme of the reaction of steam reforming of methane is shown in Equation 2.1:

$$CH_4 + H_2O \rightarrow CO + 3H_2 \qquad \Delta H^{\circ}_{298} = 205 \frac{kJ}{mol} \qquad (2.1)$$

The steam reforming of methane is an endothermic process and, therefore, requires very high temperatures. Consequently, this process is relatively energy and cost intensive. Therefore, research on alternative processes of methane reforming with economic viability prospect is gaining interests.

2.2.2 Partial Oxidation

The partial oxidation (POX) of methane is a catalytic process that involves partial oxidation of methane in the presence of catalyst, and the product of this reaction is syngas with a good H_2/CO ratio (Fathi et al., 2000). The scheme of the partial oxidation of methane is shown below in Equation 2.2:

$$CH_4 + \frac{1}{2}O_2 \rightarrow CO + 2H_2 \qquad \Delta H^{\circ}_{298} = -36.0 \frac{kJ}{mol} \qquad (2.2)$$

The partial oxidation of methane is an exothermic process. On the other hand, partial oxidation is considered an expensive process because it requires a flow of pure oxygen compared to dry reforming. Thus, there is a warning of danger that is inherent in the process of partial oxidation of methane, since the two reagents (CH_4

and O_2) can cause an explosion if the reaction is not conducted with the necessary care (Peña et al., 1996).

2.2.3 Autothermal Reforming

The autothermal reforming (ATR) of methane is a combination of both steam reforming and partial oxidation in the presence of a catalyst (Armor, 1999). Hence, this process of catalytic reforming of methane involves three reactants, viz. (CH_4, H_2O, and O_2). The scheme of the autothermal reforming of methane is given by Equation 2.3 shown below.

$$2CH_4 + \frac{1}{2}O_2 + H_2O \rightarrow 2CO + 5H_2 \qquad \Delta H^{\circ}_{298} = -36.0\,\frac{\text{kJ}}{\text{mol}} \quad (2.3)$$

The autothermal reforming of methane process is designed to save energy, because the thermal energy required is generated in the partial oxidation of methane. As this process consumes the thermal energy that it produces, it is called autothermal (Ayabe et al., 2003)

Similar to other reforming processes of methane, the main purpose of autothermal reforming is the production of syngas. The value of the H_2/CO ratio of the syngas obtained in the autothermal reforming is a function of the gaseous reactant fractions introduced in the process input. Typically, the value of H_2/CO ratio ranges between 1 and 2 (Palm et al., 2002).

2.3 Dry Reforming of Methane

Methane dry reforming (DRM) is a catalytic reaction between methane and carbon dioxide to produce synthesis gas (a mixture of hydrogen and carbon monoxide). The dry reforming of methane is given by Equation 2.4 shown below:

$$CH_4 + CO_2 \rightarrow 2CO + 2H_2 \qquad \Delta H^{\circ}_{298} = 247 \frac{\text{kJ}}{\text{mol}} \qquad (2.4)$$

Production of syngas through the DRM has recently attracted intense interest. One advantage associated with this reaction pathway compared to steam reforming or partial oxidation, is the low H/CO ratio, typically at 1, which is suitable for synthesis of oxygenated derivatives such as alcohols (Cheng et al., 2001; Hou et al., 2003) and Fischer-Tropsch synthesis (Bradford et al., 1996; Zhang et al., 2007; Bermúdez et al., 2011). The process also special interest due to its potentially friendly effect on the environment by reduces greenhouse gas emissions (Tsang et al., 1995; Edwards et al., 1996).

Cheng et al. (2001) reported that, the value of the H_2/CO ratio obtained in the DRM is considered the best product of reforming process when it comes to use the syngas produced as a raw material for the synthesis of important fuel liquids which require H_2 and CO as raw materials. On the other hand, this type of reforming process is considered relatively expensive because, being an endothermic process; it consumes a great amount of energy. From the industrial standpoint, it is more practical to develop Ni-based catalysts because of their low price, high activity at

elevated temperature, excellent thermal stability and wide availability (Kim et al., 2000).

The main disadvantage of DRM is the high thermodynamic potential to coke formation (Gadalla, & Bower, 1988; Hou et al., 2003; Souza et al., 2004). The deposition of coke on the surface of the catalyst contributes to the reduction of its longevity. Ding et al. (2001) suggested that carbon deposition was inevitable in the temperature range from 300 to 1000 ^{o}C from the thermodynamics analysis.

Process of DRM is often challenged by many factors. This reaction is characterized by several aspects such as carbon deposition leading to rapid catalyst deactivation (Olsbye et al., 1997; Batiot-Dupeyrat et al., 2008), and severe temperature gradients at high conversions due to the highly endothermic nature of the reaction (Daza et al., 2010).

It has been reported that there are various types of carbon formation on Ni-based catalysts during DRM process at least some of which may also be produced on noble metal catalysts. More specifically, there are three kinds of carbonaceous species that can form on the catalyst during methane reforming reaction (Xu et al., 2009). These are C_{α}(polymeric), C_{β}(filamentous), and C_{γ}(graphitic), respectively. Carbon deposition on catalyst results primarily from the following reactions (Gallego et al., 2008; Xu et al., 2009):

Methane decomposition:

$$CH_4 \rightarrow C_{(C)} + 2H_2 \qquad \Delta H^{\circ}_{298} = 75 \frac{\text{kJ}}{\text{mol}} \qquad (2.5)$$

CO disproportionation (Boudouard reaction):

$$2CO \rightarrow C_{(C)} + CO_2 \qquad \Delta H^{\circ}_{298} = 205 \frac{\text{kJ}}{\text{mol}} \qquad (2.6)$$

At high temperatures, the Boudouard reaction is thermodynamically limited (Bradford & Vannice, 1999), suggesting that it is desirable to operate at high temperature. However, methane decomposition is favored at high temperature, meaning that there is a need to optimize the temperature to minimize the thermodynamic driving force for carbon deposition from these two reactions. Catalysts that can inhibit carbon formation kinetically at condition where carbon formation is thermodynamically favorable are desirable.

2.4 Catalyst

The behaviour of supported metallic catalysts in the CH_4 reforming with CO_2 depends on several interrelated factors such as the nature of the metal, the support type, the metallic particle size and the characteristics of the metal-support interface (Zhang et. al., 1996; Bitter et. al., 1997; Tsipouriari et. al., 1994; Ricchardson & Paripatyadar, 1990; Qin & Lapszcewiz, 1994).

Group VIII metals, usually base metal catalysts (Ni, Co, and Fe) as well as noble metal catalysts (Pt, Ru, Rh, and Pd) are active for the dry reforming reaction. These are usually dispersed on various oxide supports. In the reforming reaction, the catalysts contain one or more metallic active species deposited on a support material. The metals species interact with the support to form of metal-support interaction. Alumina (γ-Alumina, α-Alumins) is widely used as support; or as bi-supports in the form of magnesium aluminate, calcium aluminate. In addition, ceria, magnesia, pervoskites, and zirconia are also commonly employed as support materials.

The selection support plays the important role in determining the activity and stability of a catalytic material. The main function of the support metal is to increase the surface area of the active component. Catalytic activities generally increase with increasing catalyst surface area, but a linear relationship cannot be expected since the reaction is often strongly dependent on structure of the catalyst surface.

Section 2.4.1 reviews the performance of various metals and supports on the dry reforming activity. The modification of metal-based catalyst by promoters in dry reforming will also be examined along with their application in the improvement of catalyst deactivation.

2.4.1 Base Metal Catalyst

Li et al. (2005) showed the superiority of Ni over Pt and Pd in alumina-supported systems for dry reforming of methane. Other studies undertaken by Rostrup-Nielsen (1973), Engler et al. (1991), and Murata et al. (2004) revealed that Ru and Re exhibited activity comparable to Pt, Pd and Rh during dry reforming of methane. Interestingly, Wang et al. (2004) also suggested that Ni and Re give higher conversions than Ru and Rh in dry reforming of methane. Significantly, for dry reforming of methane, there is a clear indication that Ni is indeed the most active species, whilst Pd and Pt also gave good conversions. (Souza et al., 2004; Fidalgo et al., 2010).

When metals are deposited on zirconia (ZrO_2) or ceria (CeO_2) supports, Eltejaei et al. (2012) and Özkara-Aydlnoğlu et al. (2009) also found that Pt, Pd and Ni were more active than other metals studied under methane dry reforming. Moreover, for MgO-supported catalysts, Qin and Lapszewics (1994) showed that Ru, Rh, and Ir gave higher and more stable activity among the noble metals.

The effect of metal loading on conversion during dry reforming has also been studied by a number of investigators. Xu et al. (2001) found that methane conversion increased when the Ni reached an optimum level at 2.4 wt. %. They reported that, the Ni content at 4 % resulted in lower conversion while further addition to 20 % did not yield any significant improvement.

Yanhui and Diyong (2001) reported similar behavior on Ni/Al_2O_3 for steam reforming of n-octane. The catalyst activity increased with increased nickel content in a range between 1-5 wt.%, while the improvement in activity was not perceptible with further addition in nickel loading at above 5 wt.%. It was revealed that at the optimum conversion, the nickel surface area was the highest. Overloading of catalyst will be cause particle agglomeration and formation of aluminates leading to poorer dispersion and unstable catalyst.

2.4.2 Effect of Support

The activity of various materials used as supports in hydrocarbon dry reforming catalysts studies by many researchers. As may be seen, most support comparison studies employed active components obtained from Group VIII metals. Alumina (Al_2O_3) was often used as the support due to its low cost, high surface area and stable mechanical properties.

The nickel-based catalyst the use of Al_2O_3 as a support appeared in general to give higher activity during methane dry reforming over other unmodified, single-component supports. For lower temperature range (< 600 ^{0}C), Matsumura et al. (2004) and Kusakabe et al. (2004) however reported that Ni/ZrO_2 showed better activity and stability than both Ni/Al_2O_3 and Ni/SiO_2.

In an effort to improve the performance of ZrO_2, several researchers have added cerium oxide (CeO_2) to this support. The accompanying enhancements were credited to the role of CeO_2 in stabilizing metal dispersion (Kusakabe et al., 2004). In contrast, Laosiripojana and Assabumrungrat (2005) found lower conversion in Ni/Al_2O_3, although accompanied with less carbon deposition, compared to $Ni/CeZrO_2$. They argued that dry reforming activity of Ni/Al_2O_3 is strongly inhibited by high hydrogen presence.

Nakagawa et al. (2003) studied the effect of support material in nickel-based catalysts for dry reforming of CH_4. The methane conversion in the decreasing order is: $Al_2O_3 > Y_2O_3 > TiO >> MgO > SiO_2 > La_2O_3$. As illustrated in Figure 2.1, both product concentrations and CH_4 conversion were influenced by the choice of support.

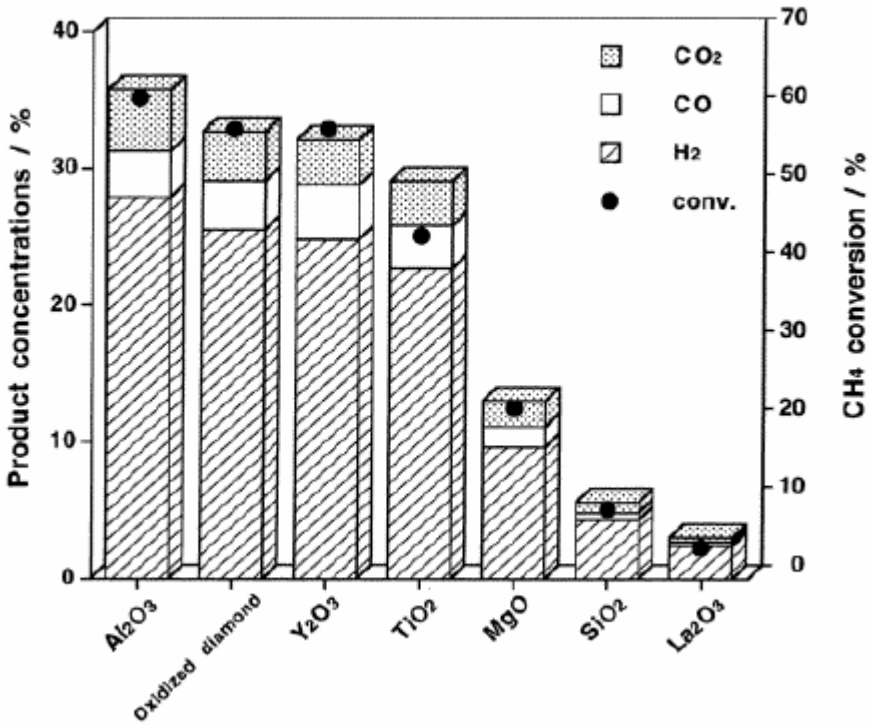

Figure 2.1: Effect of supports on CH_4 conversion and product concentrations for the dry reforming of CH_4 over nickel-loaded catalysts. Reaction conditions: temperature, 600 ^{0}C; reaction time, 0.5 h; CH_4:CO_2:Ar ratio, 1:3:5.

(Sources: Nakagawa et al., 2003)

Liguras et al. (2003) investigated the effect of ruthenium (Ru) metal dispersed with equal loading on different supports, i.e. Al_2O_3, MgO and TiO_2. The high activity of Al_2O_3 was assigned to the ability of Ru particles to disperse on this type of support. The measured dispersion of Ru on Al_2O_3 was 21 % compared to 7 and 2 % for TiO_2 and MgO respectively. The Ru/Al_2O_3 catalyst was aslo reported to yield higher selectivity toward reforming products. The poorly-dispersed, MgO-supported catalyst however resulted in a moderate and stable activity probably due ti its bacis nature which prevented production of ethylene and hence, recuded coke formation.

2.4.3 Effect of Promoter on Ni-Based Catalysts

In order to improve the stability and the carbon resistance of nickel-based catalysts, the supports metal have been modified by adding the promoter, mainly by addition of alkali and alkaline earth metal oxides as well as rare earth oxides (Wang et al., 2001; Dong et al, 2002; Takeguchi et al., 2003). The rare earth oxides have a high oxygen storage capacity and can absorb or release oxygen reversibly in responding to the oxygen concentration in the gas-phase. Their presence shows advantage effects on the catalyst performance, such as improving the dispersion of the active species and delaying the transition of alumina support (Soria et al., 1996; Morterra et al., 1996). It has been demonstrated that the addition of ceria as a promoter in the Ni/Al_2O_3 catalyst can enhance the activity, stability and resistance of carbon deposition in CH_4 reforming with CO_2 (Wang & Lu, 1998; Cheng et al., 2001).

Further studies by Zhang et al. (1994), Cheng et al. (1996), and Choudhary et al. (1996) found that Ni supported on $CaO\text{-}Al_2O_3$ exhibited higher reforming activity rather than Ni/Al_2O_3, while Lodeng et al. (1997) and Lu et al. (1999) found the addition of CaO increased the coke formation of Ni/Al_2O_3. But Horiuchi et al. (1996) indicated that excess impregnated Ca reduced the activity of $Ni/\gamma\text{-}Al_2O_3$. Hou et al. (2003) reported that, the Ca-promoted $Ni/\alpha\text{-}Al_2O_3$ the reforming activity was increased greatly and the coke formation rate changed slightly compared with pure $Ni/\alpha\text{-}Al_2O_3$. They also found that the coke formation rate decreased when the Ca/Ni reached at ≤ 0.08, mol ratio. They reported, the Ca/Ni at ≥ 0.1, mol ratio resulted in

higher coke formation. So, the influence of Ca on the activity of Ni/α-Al_2O_3 changed with the amount of Ca added.

Yang et al. (2010) studies the promotional effect of La_2O_3 and CeO_2 on Ni/γ-Al_2O_3 catalysts for CO_2 reforming of CH_4. They reported that the CH_4, CO_2 and total carbon conversion decreased with La loading increasing from 0 to 3%, and did not clearly change with La loading increasing from 3 to 9%. However, the carbon deposition on the 10%Ni/La_2O_3-γ-Al_2O_3 catalyst decreased with increased La loading, while the carbon deposition did not clearly change with La loading increasing from 3 to 9%. They also showed that the carbon deposition on 10%Ni/3% La_2O_3-γ-Al_2O_3 catalyst decreased more than 50% compares with that of 10%Ni/La_2O_3-γ-Al_2O_3 catalyst at the same reaction condition. This was favorable to improve 10%Ni/La_2O_3-γ-Al_2O_3 with La loading of 3%. They also reported that the CeO_2-promoted Ni/γ-Al_2O_3 catalysts for CH_4 reforming with CO_2 similar with La_2O_3.

CHAPTER III

METHODOLOGY

3.1 Introduction

This chapter provides a list of chemicals employed for the preparation catalyst, including their supplier, grade, physical and chemical properties. Additionally, the operational procedures of the catalyst characterization instruments also presented in this chapter. The first stage of this experiment work is the synthesis of catalyst. The catalysts comprised of the Al_2O_3 support, 10%Ni/90%Al_2O_3 and 3%La-10%Ni/87%Al_2O_3 was prepared. All the catalysts wase characterized using X-ray Fluorescense (XRF), Fourier Transform Infrared Spectroscopy (FTIR), Brunauer, Emmett and Teller (BET) isotherm, and X-ray Diffraction (XRD) in order to obtain their physicochemical properties. The result obtained was compared with other previous researches. Finally, conclusions will be drawn based on the findings

obtained from this study. The overall experimental work was summarized in Figure 3.1.

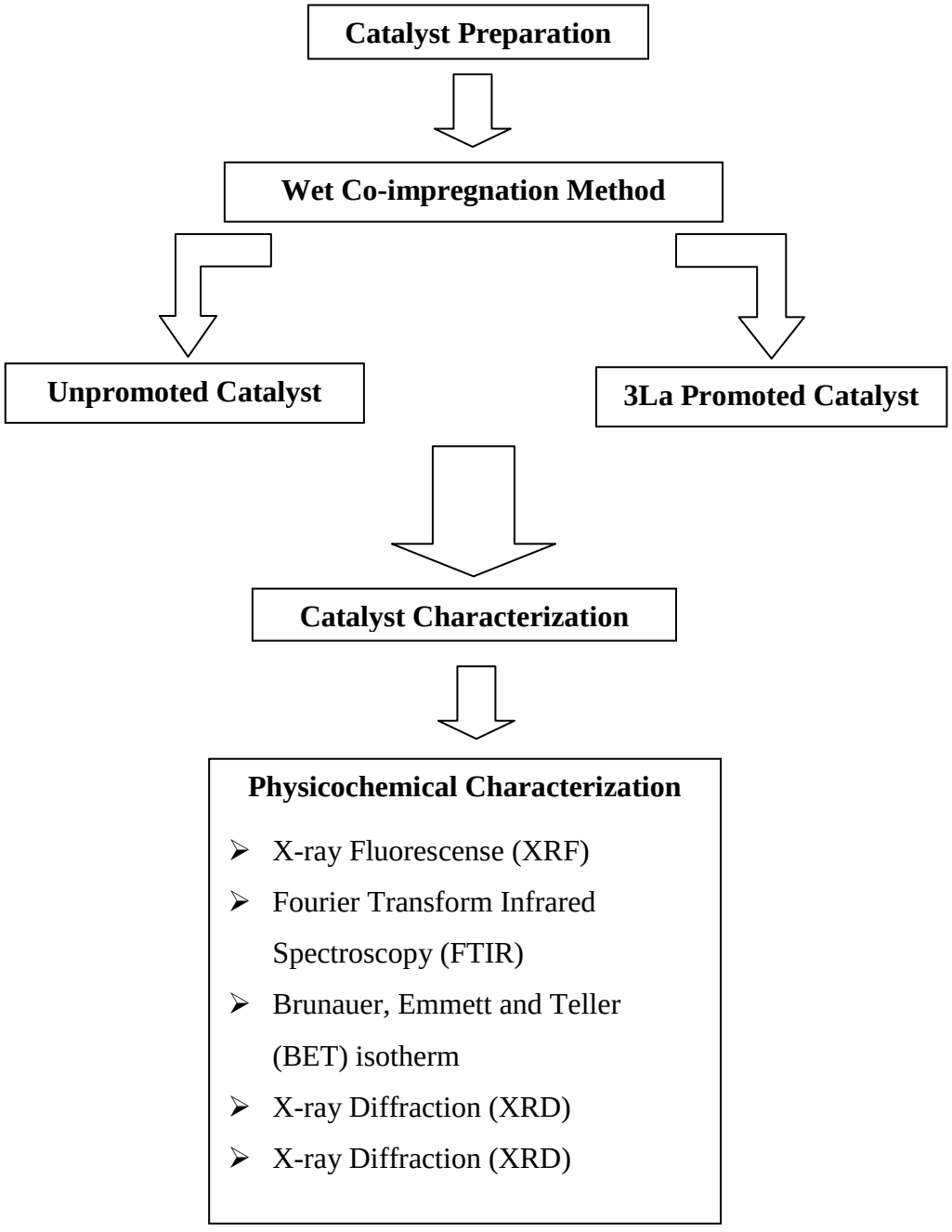

Figure 3.1: Flow chart of overall experimental work.

3.2 Materials And Chemicals

All chemicals and material used in this study are provided in Table 3.1.

Table 3.1: List of chemicals.

Chemicals	Molecular Formula	Supplier	Molecular Weight (g/mol)	Purity (%)
Aluminium Oxide	Al_2O_3	Sigma-Aldrich	101.96	99
Nickel (II) Nitrate Hexahydrate	$Ni(NO_3)_2.6H_2O$	Sigma-Aldrich	290.79	98.5
Lanthanum nitrate solution	$La(NO_3)_3$	Sigma-Aldrich	324.92	99.9
Methane	CH_4	Sigma-Aldrich	16.04	99.995

3.3 Catalyst Preparation

3.3.1 Unpromoted Catalyst

The catalysts used in this study will be prepared by wet co-impregnation method described by Hou et al. (2003). Al_2O_3 was impregnated in solution of $Ni(NO_3)_2.6H_2O$ (Sigma-Aldrich), followed by 3 h of constant stirring on a magnetic stirrer. Stirring rate was adjusted to a certain speed (7 on a 10-speed unit Magnetic Stirrer) which provides adequate mixing of Al_2O_3 support particles in the slurry solution for homogenous distribution. The resulting solution was dried overnight in an oven at 120 ^oC. The calcination of the product was carried out by 5 $^0C\ min^{-1}$

ramping to 800 ^{o}C and holding at that particular temperature for for 6 h with continuous air flow at 200 ml min^{-1} (Yang et al., 2010).

3.3.2 3La Promoted Catalysts

The promoted 3%La-10%Ni/87%Al_2O_3 catalyst was prepared by wet co-impregnation. Initialy, an aqueous $La(NO_3)_3$ solution was prepared based on the required amount of lanthanum nitrate to give the desired metal loading. Then, Al_2O_3 was transferred to the $La(NO_3)_3$ solution, followed by gentle stirring on a magnetic stirrer for 3 h at a stirrer speed scale of 7. Subsequently, the samples was dried overnight in an oven at 120 ^{o}C for moisture removal. The dried solid was impregnated with the required quantity of an aqueous $Ni(NO_3)_2$. $6H_2O$ solution under conditions similar to those of the first impregnation. The final product was calcined in an oven using air flow under varying thermal condition, i.e. temperature (600 ^{o}C – 800 ^{o}C), and holding time (2 – 6 h) (Yang et al., 2010).

3.4 Catalyst Characterization

Catalyst characterization provides useful information on the physicochemical attributes of the catalyst. Analytical techniques such as spectroscopic, microscopic, diffraction or chemical analysis can be effectively used to investigate the catalyst

surface and bulk properties. This section describes the fundamental concepts of various characterization techniques employed for this study.

Most substances used as catalyst supports are porous in nature. These materials contain deep and complicated network of pores accountable for internal surface area. Surface area is obviously a key property of a porous material. Despite the fact that support surface are not uniform in nature, higher surface area is often a good indication of a more active catalyst. In such a case, metal crystallites can be more homogenously distributed on the maximum possible surface and hence, an increase in adsorption sites for reactant molecules.

3.4.1 Fourier Transform Infrared (FTIR)

FTIR is most useful for identifying chemicals that are either organic or inorganic. It can be utilized to quantify some components of an unknown mixture. It can be applied to the analysis of solids, liquids, and gases. FTIR is perhaps the most powerful tool to use in this research for identifying types of chemical bonds (functional groups), spectrum analysis and properties of solid catalyst. The wavelength of light absorbed is characteristic of the chemical bond as can be seen in this annotated spectrum. By interpreting the infrared absorption spectrum, the chemical bonds in a molecule can be determined.

The analysis on the samples of support, unpromoted and 3La promoted catalyst was conducted by FTIR (Thermo Electron Technology) using KBr disk pellet technique. The wavelength used was in range 500 – 4000 cm^{-1}.

3.4.2 X-ray Diffraction (XRD)

The crystalline phases and structure of the Al_2O_3, 10%Ni/Al_2O_3 and 3%La-10%Ni/Al_2O_3 catalysts was determined using X-Ray Diffraction (XRD) techniques. This method is based on the fact that every crystalline material has its own characteristics diffractogram. Additionally, from this technique the mean crystallite size in the range 3 to 50 nm can be estimated. When the crystalline size is smaller than 3 nm, the X-ray pattern would show a broad and diffuse, or even absent, diffraction lines. On the other hand, in crystalline larger than 50 nm, the change in the line shape would not be apparent (Anderson & Pratt, 1985). XRD patterns was acquired on a Siemens D5000 goniometer using CuKα radiation ($\gamma = 1.542\ \dot{A}$) at 40 kV and 30 mA.

The catalyst samples were initially crushed to a fine powder (< 100μm). The specimens was placed on a glass specimen holder and pressed using a glass slide. Scanning of samples was performed starting from 5^o to 80^o at a speed of 3^o min^{-1}. All the samples were dried before diffractograms are measured. A peak obtained from the analysis was identified using the Hanawalt search match interpretation method to reveal the type of phases present (JCPDS, 1983).

3.4.3 Brunauer-Emmett-Teller (BET)

Surface area, pore size and pore volume are among the most fundamentally important properties of a catalyst because they determine the measure of its internal surface available to accommodate active sites. Despite the fact that support surface are not uniform in nature, higher surface area is often a good indication of more active catalyst. Brunauer-Emmett-Teller (BET) method is a common technique used to measure solid surface area. In a pioneering work, Langmuir developed a relationship between the amount of adsorbed gas and its equilibrium pressure at constant temperature (Langmuir, 1916).

The Langmuir''s model for a monomolecular adsorption is generally expressed by Equation 3.1:

$$\theta = \frac{\alpha_o \mu}{n\left(1+\frac{\alpha_o \mu}{n}\right)} \qquad (3.1)$$

Where:

θ = fraction of surface of covered by adsorbed molecules,

α_o = ratio of number of gas of inelastic collisions resulting in absorption to total number of collisions of gas molecules on the surface,

n = number of adsorbed molecules desorbing in unit area of the surface,

μ = number of molecules colliding in unit time with a unit area of the surface.

Based on Langmuir's monomolecular model, Brunauner, Emmet and Teller derived an expression for multilayer adsorption, given by Equation 3.2:

$$\frac{\mathrm{P}}{\mathrm{V}(\mathrm{P_S}-\mathrm{P})} = \frac{1}{\mathrm{cV_m}} + \frac{(\mathrm{c}-1)\mathrm{P}}{\mathrm{cV_m P_S}} \quad (3.2)$$

Where:

P = gas pressure,

P_S = saturation pressure of adsorbed gas,

V = volume of gas adsorbed,

V_m = volume of adsorbed gas corresponding to monolayer coverage,

c = a constant, characteristic of the adsorbate.

A plot of $\frac{P}{V(P_S - P)}$ versus $\frac{P}{P_S}$ provides a straight line with the intercept and slope of $\frac{c-1}{V_m c}$ and $\frac{1}{V_m c}$ respectively from which the volume of adsorbed gas corresponding to monolayer coverage, V_M, and c will be calculated. The preferred range of $\frac{P}{P_S}$ for best results is 0.05 to 0.4 (Emmett, 1954). The surface area per weight unit can subsequently be computed by Equation 3.3.

$$\mathrm{S_A}(\mathrm{m^2 g^{-1}}) = \left(\mathrm{V_M}, \frac{\mathrm{cm}^3}{\mathrm{g}}\right)\left(\frac{6.023 \times 10^{23} \text{ molecules}}{21400 \text{ cm}^3 \text{ STP}}\right)\left(\frac{\text{cross} - \text{sectional area}, \mathrm{m}^2}{\text{molecule}}\right) \quad (3.3)$$

Where;

S_A = surface area of solid,

V_m = volume of adsorbed gas corresponding to monolayer coverage.

And for N_2 the usual cross-section area is 16.2 $\dot{A}^2$ ($1\dot{A}^2 = 10^{-20} m^2$) (Gregg & Sing, 1991).

Firstly, around 0.25g of freshly calcined catalyst was packed in the U-sample tube. The sample was degassed at 300 ^{0}C at overnight and cool down to ambient temperature. Once, TCD signal has stabilized, the sample tube was quickly immersed in a flask fill up with liquid N_2. As a result, nitrogen will be physisorbed on the support surface. And then, the adsorption has reached at equilibrium, the sample was be shifted back to ambient temperature by swapping the liquid N_2 flask with a water fill up in flask. The adsorption of nitrogen species was detected by changes in the TCD signal as typically shown in Figure 3.2. Consequently, the surface area will be determined by Equation 3.3. The technique encompasses external area and pore area evaluations to determine the total specific surface area in m^2/g yielding important information in studying the effects of surface porosity and particle size in many applications.

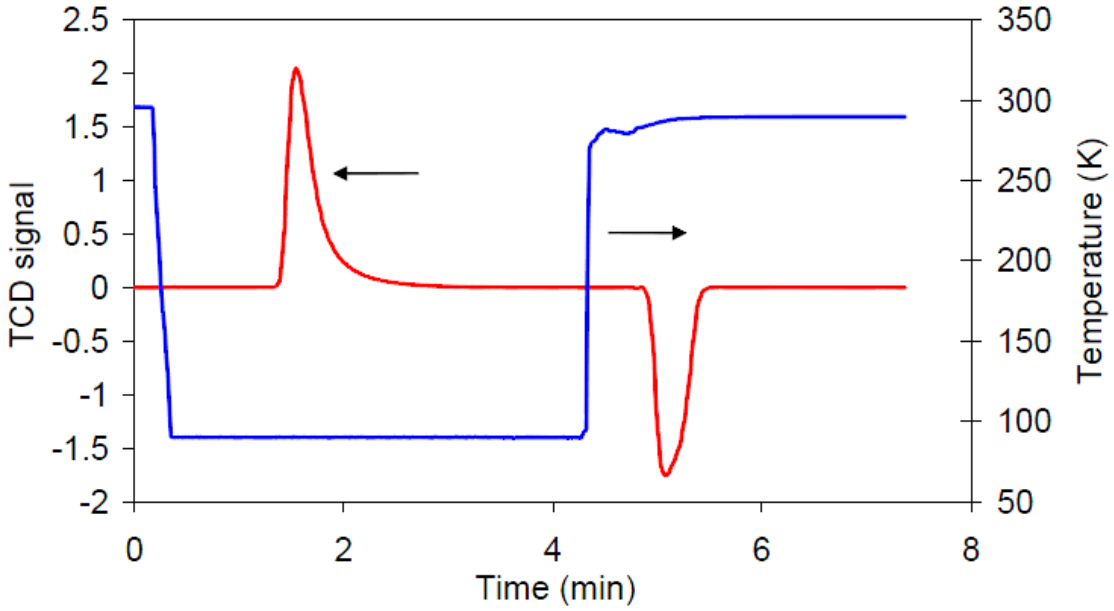

Figure 3.2: Typical adsorption peaks during BET measurement.

(Sources: Cheng et al., 2001)

CHAPTER IV

RESULT & DISSUSSION

4.1 Introduction

This chapter discusses based on the data from the experimental work that had been carried out. The result is described in the analysis of the physicochemical characterization for the catalysts comprised of the Al_2O_3 support, unpromoted (10%Ni-Al_2O_3) and 3La promoted catalyst (3%La-10%Ni-Al_2O_3). The physicochemical study of the samples was characterized using X-ray Fluorescense (XRF), Brunauer, Fourier Transform Infrared Spectroscopy (FTIR), Emmett and Teller (BET) isotherm, and X-ray Diffraction (XRD) was described in below. Finally, conclusions were drawn based on the findings obtained from this study.

4.2 Physicochemical Characterization

It is reported in the literature that the addition of lanthanum as a promotion improved catalyst ensured resilience against carbon deposition in dry reforming processes. However, there has been no attempt to systematically evaluate the behavior and influence of lanthanum, loading as a precursor to obtain quantitative and qualitative insights, as most of the limited published studies used lanthanum as a support under dry reforming reaction. In what follows, this study aims to enhance the knowledge about the promotional effect of lanthanum with an attempt to provide leadership for commercializing the dry reforming process. This is intended to be achieved through studying the characterisation of the designed catalyst as provided in this chapter.

In this section, the effect of the La promotion on the physicochemical properties was investigated through the outcomes of four main techniques. Firstly, the main metals presented in calcined catalyst of unpromoted (10%Ni-Al_2O_3) and 3La promoted catalyst (3%La-10%Ni-Al_2O_3) were examined under XRF method. Besides that, the functional group or typed of chemical bonding in the samples was identified under FTIR analysis. Then, discussion of the N_2-physisorption result reflects the changes in surface area and pore size. Last but not least, the major crystalline phases and bulk-phase in the catalyst was examined under XRD analysis.

4.2.1 X-Ray Fluorescense (XRF) Analysis

The main metal composition presented in calcined catalyst of 10 wt.% Ni-Al_2O_3 (unpromoted catalyst) and 3 wt.% La-10 wt.% Ni-Al2O3 (3La promoted catalyst) measurement by The X-ray Fluorescense (XRF) method. The XRF data for calcined catalysts of the unpromoted and 3La promoted catalyst are tabulated in Table 4.1.

Table 4.1: XRF analysis for main metal presented in unpromoted and 3La promoted catalyst.

Metal	Al	Ni	La	O_2 (balance)
Content (wt %)	50.64	9.5	-	39.86
	50.37	9.3	2.5	37.83

From Table 4.1, the final nickel content in the calnined 10Ni/Al_2O_3 (unpromoted catalyst) was approximately 10 wt.% of the initial loading, which further reduced to 9.5 wt.% after calcined at 1073 K for 6h. This indicates that there is loss of the nickel during calcination of the catalyst. Besides that, the final lanthanum content in the calcined 3La-10Ni/Al_2O_3 (3La promoted catalyst) also loss during the calcination from 3 wt.% of the initial during preparation of Lanthanum as promoter in Ni-based catalyst through wet impregnation to 2.5 wt.% of the final

lanthanum content in 3La promoted catalyst. As it can be seen the final result found to be in a good agreement with the intended composition.

4.2.2 Fourier Transform IR (FTIR) Spectrum Analysis

The Fourier Transform IR (FTIR) spectra of the support catalyst which Al_2O_3 and calcined catalysts for unpromoted and 3La promoted catalysts at 1073 K for 6 h are depicted in Figure 4.1. The samples are sensitive absorption around region 4000 – 500 cm^{-1} but the sensitive absorption of the samples was divided into the different sensitive absorption regions. The large different sensitive absorption was divided into two infrared spectrum region which around 3700 – 3000 cm^{-1} and 1500 – 500 cm^{-1} as showed in Figure 4.1.

This intense vibration in the region indicates the existing of nickel metal dispersion in the unpromoted samples and also, the existing of lanthanum metal dispersion in the promoted catalyst. For sample Al_2O_3, which is supported catalyst has characteristic broad absorption bands recorded at around 3660 – 3450 cm^{-1} is associated to the presence of hydroxyl, OH bonded. The band at 3539 cm^{-1} corresponds to the OH^- groups bounded in linear forms. Besides that, the band at 3415 cm^{-1} to the OH^- group bounded in bridged forms. The bands at region 978 – 526 cm-1 correspond to Al-O bonded. This strong vibration is assigned to Al-O asymmetric stretching vibration. These findings also stated in co-precipitated iron-containing catalysts (Fe-Al_2O_3, Fe-Co-Al_2O_3, Fe-Ni-Al_2O_3) for methane

decomposition at moderate temperatures for calcined catalysts through by Reshetenko et al., (2004).

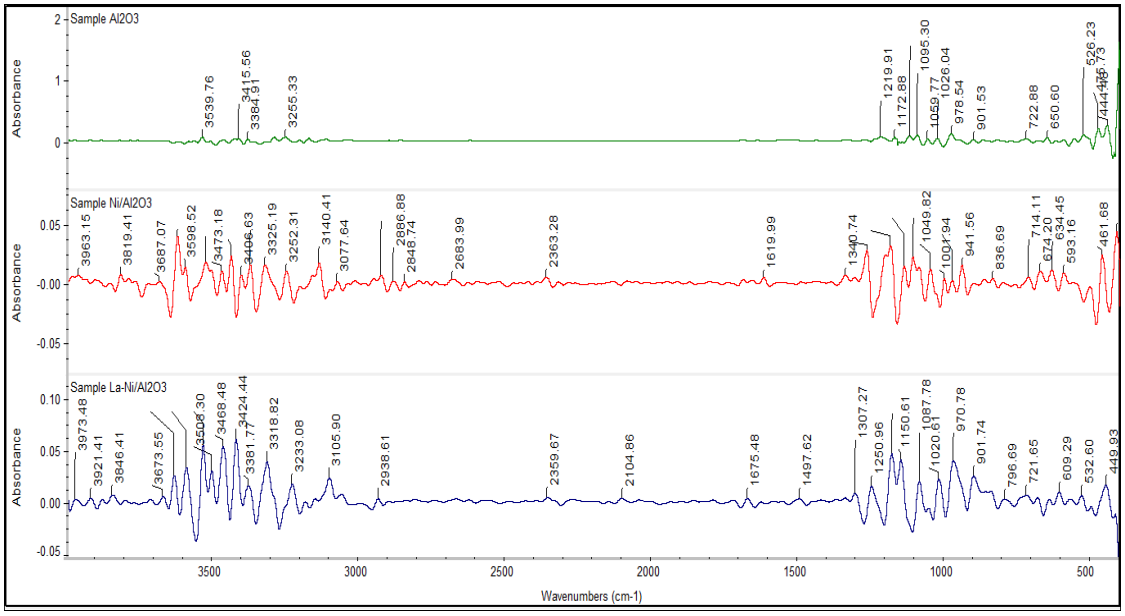

Figure 4.1: FTIR spectrum of the support catalyst and calcined unpromoted and 3La promoted catalyst at 1073 K for 6 h.

The characteristic vibration band starts from 1000 – 500 cm^{-1} with the highest peak intensity at 970.8 cm^{-1} and the lowest peak intensity at 634.5 cm^{-1}. It is observed that the band recorded at 901. 7 cm^{-1} of 3La promoted catalyst can be assigned to Al-O symmetric stretching has less intensity compared to asymmetric stretching of Al-O bond compared to unpromoted catalyst which the band recorded at 941.5 cm^{-1}. This is likely as the probability of symmetric stretching of Al-O bond is less compare to asymmetric stretching and bending (Liguras et al., 2003). Another

intense and sharp bend happened at 796.7 cm^{-1} which indicates the presence of double ring in the 3La promoted catalyst.

From Figure 4.1, it can be observed that unpromoted and 3La promoted catalyst sample also show the characteristic IR bands, in the range of discussed in Al_2O_3 support catalyst sample. IR spectra of sample Al_2O_3 support catalyst show characteristic IR band at frequencies similar to those other sample which unpromoted and 3La promoted catalyst. Other samples, unpromoted and 3La promoted catalysts also have the quite similar peak with almost the same intensity which is around 3660 – 3450 cm^{-1} is associated to the presence of hydroxyl, OH bonded. Besides that, also similar peak with almost the same broad absorption bands recorded at around 978 – 526 cm^{-1} correspond to Al-O bonded. This finding showed that strong vibration is assigned to Al-O asymmetric stretching vibration in unpromoted and 3La promoted catalysts as Al_2O_3 support catalyst.

There are some differences between samples unpromoted and 3La promoted catalyst. The different in the amount of peaks in the region is because of different metal composition of in both samples. In sample unpromoted catalyst, the fewer peak shows the presence of nickel loaded in supported catalyst (Al_2O_3). The FTIR spectra of the calcined unpromoted catalyst of 10 wt.%-Al_2O_3 contain an absorption band at 593.1 cm^{-1} characterizing Ni-O strerching vibrations. Vibrations at 941.6 and 1001.9 cm^{-1} correspond to vibrations Ni-O-H. Bands at 3406.6, 3473.2 3598.5 cm^{-1} belong to stretching vibrations of –OH group. The absorption band about 1620 cm^{-1} corresponds to vibration δ-H_2O. The appearance of absorption bands in the absorption range of hydroxyls indicates the formation of a metal hydroxide during

wet impregnation (Reshetenko et al., 2004). Note that the IR spectrum in this region is similar to that of hydroxide with the bayerite structure. This means that this samples contains a large amount of the structural supported catalyst Al_2O_3 (up to 50 wt.%) (Frederiskson, 1954).

3La promoted catalyst in Figure 4.1 also have the quite similar peak with almost the same intensity unpromoted catalyst. Meanwhile in sample 3La promoted catalyst, there is more peak vibration shown due to the presence of Lanthanum metal act as promoted in Ni-based catalyst. In addition to that, a band is observed at 609.3 cm^{-1} corresponds to Ni-O-La vibration in 3La promoted catalyst.

Thus it can be concluded those IR spectra of sample support catalyst (Al_2O_3) and other modified catalyst match quite closely, indicating the presence of similar structural unit and formation of identical chemical moieties of the unpromoted and 3La promoted catalysts, but the pattern shown in supported catalyst have some differences between samples unpromoted and 3La promoted because different metal composition of in both samples.

4.2.3 N_2 – Physisorption Analysis

The analysis for the profile of absorption and desorption for the catalyst gives important details about surface area, pore volume and pore diameter distribution. In this study, the isothermal adsorption and desorption of N_2 at -196 ^oC (77 K) were

measured as function of the change in relative pressure (P/P_0). There are six main categories classified in these isotherm profiles known as standard isotherms as shown in Figure 4.2a. Types I – V were initially established by Brunauer et al., in 1940 which was subjected to further enhancement carried out by de Boer (1958) and Gregg and Sing (1982).

In study, the isothermal profiles for the unpromoted and 3La promoted catalysts were found to be almost identical, as described in Figure 4.2a and b. This suggests a no apparent effect for the addition of La to the unpromoted catalyst and is investigative of the *Type IV* isotherm shown in Figure 4.3a. This type of isotherm is known to have capillary condensation in mesopores with high energy of adsorption (Condon, 2006). Moreover, the isothermal profile also provides supplementary information about pore geometry. The hysteresis loops may be more precisely described as *Type H1* based on the new classification recommended by the International Union of Pure & Applied Chemistry (IUPAC) as shown in Figure 4.2b (Lowell, 2004; Aligizaki, 2006). These types of hysteresis loop represents material containing cylindrical pores or spheroidal particles with reasonably uniform size (Lowell, 2004; Aligizaki, 2006).

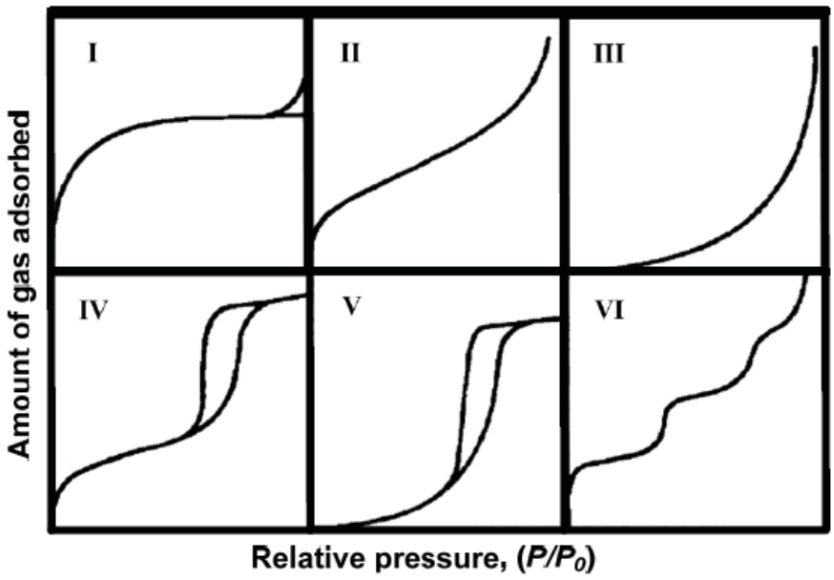

Figure 4.2a: Standard isotherms for absorption and desorption profile.

(Source: Gregg & Sing 1982)

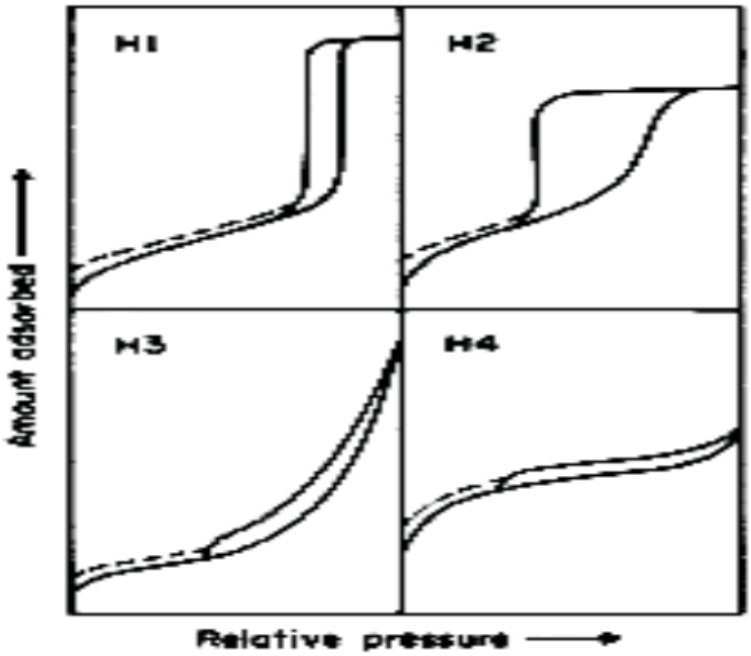

Figure 4.2b: The New classification IUPAC for hysteresis loops.

(Source: Sing et al. 1985)

The simulated isotherms for nitrogen adsorption and desorption profile for unpromoted and 3La promoted catalysts at 77 K are shown in Figure 4.3a and b, respectively. The BET surface areas of all material were calculated from the simulation isotherms for nitrogen adsorption and desorption profile in Figure 4.3a and b. The BET surface areas have two different pressure ranges which using the consistency criteria (Wang & Lu, 1998) and standard pressure range. The simulation isotherms for nitrogen adsorption profile for unpromoted and 3La promoted catalysts were tabulated in Table 4.2a and b, respectively.

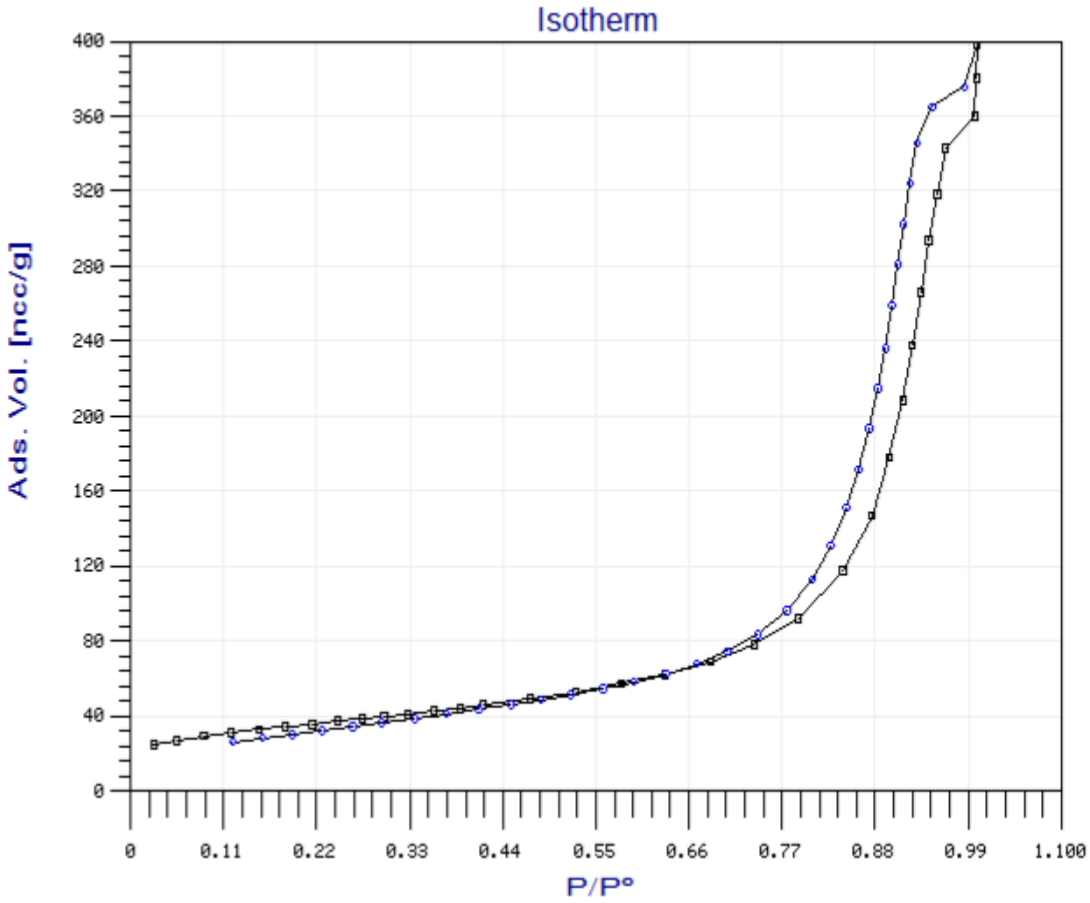

Figure 4.3a: N_2 adsorption and desorption profile for unpromoted catalyst.

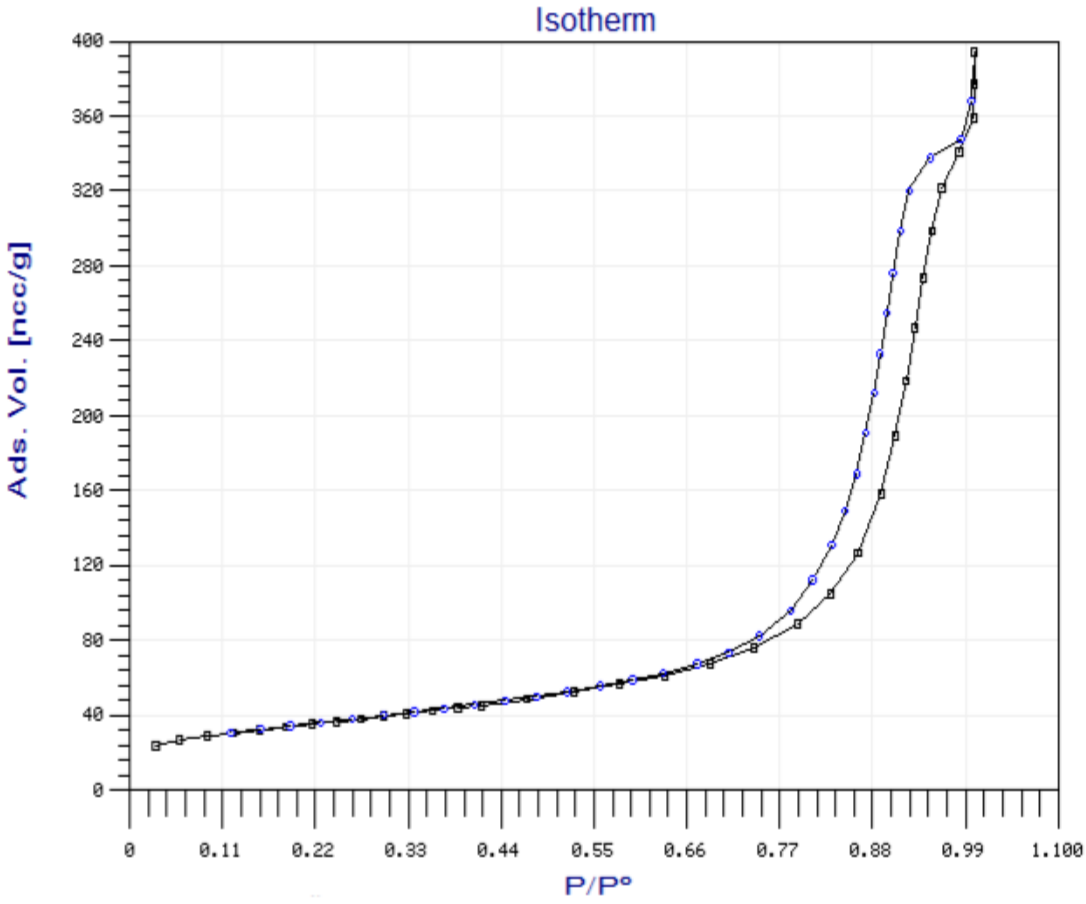

Figure 4.3b: N_2 adsorption and desorption profile for 3La promoted catalyst.

Table 4.2a: Simulation isotherm of nitrogen adsorption for unpromoted catalyst**.**

Pressure, P	Pressure Saturation, Ps	P/Ps	Ps - P	V(P-Ps)	P/V(P-Ps)
41.869	757.8	0.055251	715.931	5178.059	0.00808585
65.758	757.7	0.086786	691.942	5004.556	0.01313963
90.447	757.6	0.119386	667.153	4825.266	0.01874446
114.57	757.6	0.151228	643.03	4650.794	0.02463451
138.83	757.6	0.18325	618.77	4475.33	0.03102118
162.67	757.5	0.214746	594.83	4302.181	0.03781105
185.03	757.4	0.244296	572.37	4139.736	0.04469608
207.02	757.4	0.27333	550.38	3980.691	0.05200605
227.21	757.5	0.299947	530.29	3835.388	0.05924043

Table 4.2b: Simulation isotherm of nitrogen adsorption for 3La promoted catalyst.

Pressure, P	Pressure Saturation, Ps	P/Ps	Ps - P	V*(P-Ps)	P/V*(P-Ps)
23.338	762.4	0.030611	739.062	5452.0929	0.00428056
45.075	762.4	0.059123	717.325	5291.7381	0.008518
70.014	762.4	0.091834	692.386	5107.762	0.01370737
93.806	762.4	0.12304	668.594	4932.2474	0.01901892
117.68	762.4	0.154355	644.72	4756.1278	0.02474282
141.84	762.3	0.186068	620.46	4577.1607	0.03098864
164.88	762.2	0.216321	597.32	4406.4559	0.03741783
186.71	762.1	0.244994	575.39	4244.6773	0.04398685
208.83	762.1	0.274019	553.27	4081.4971	0.05116505
229.544	762.1	0.301199	532.556	3928.689	0.05842763

In this study, the BET surface area was calculated based on standard pressure range. According to standard pressure range including between 0.05 and 0.3 which $\left(0.05 < \frac{\mathrm{P}}{\mathrm{P_S}} < 0.3\right)$. Although this equation $\frac{\boldsymbol{P}}{\boldsymbol{V(P_S - P)}} = \frac{\boldsymbol{1}}{\boldsymbol{cV_m}} + \frac{\boldsymbol{(c-1)P}}{\boldsymbol{cV_m P_S}}$, the graph of $\frac{P}{V(P_S - P)}$ versus $\frac{P}{P_S}$ was plotting based on the standard pressure range in order to determine the BET surface area are shown in Figure 4.4.

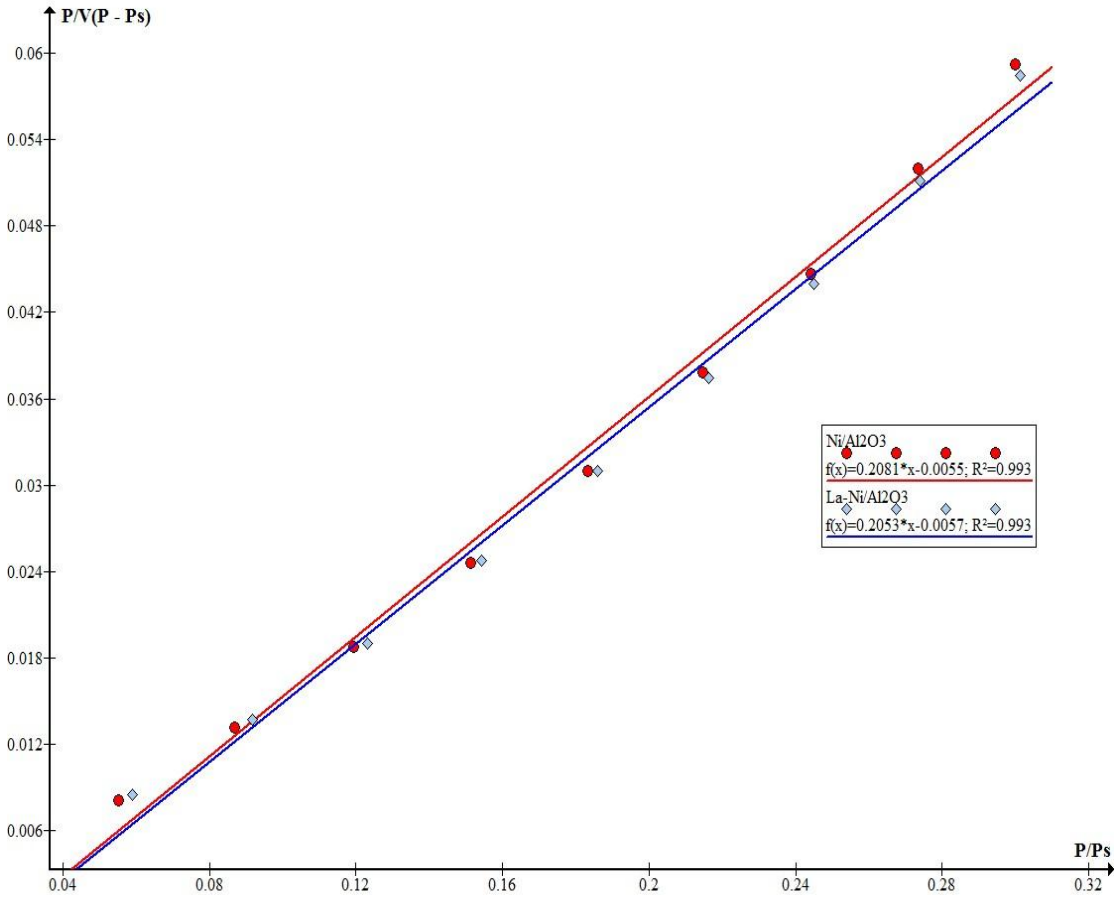

Figure 4.4: Graph of P/V (P – P_S) versus P/P_S for unpromoted and 3La promoted catalysts.

Figure 4.4 shows the graph of $\frac{P}{V(P_S - P)}$ versus $\frac{P}{P_S}$ for unpromoted and 3La promoted catalysts. In this figure, a red line as referring to unpromoted catalyst and a blue line as referring to 3La promoted catalyst. A plotting of $\frac{P}{V(P_S - P)}$ versus $\frac{P}{P_S}$, give a straight line for unpromoted and 3La promoted catalysts with the intercept and slope of $\frac{c-1}{V_m - c}$ and $\frac{1}{V_m c}$ respectively. Based on the simulation isotherm for nitrogen adsorption, a value constant for characteristic of the adsorbate (c) are 15427.58 and 15790.15 for unpromoted and 3La promoted catalysts respectively. According to the slope and value of c for unpromoted and 3La promoted catalysts, volume of adsorbed gas corresponding to monolayer coverage,V_m was calculated are 0.0003115 $\frac{\text{cm}^3}{\text{g}}$ and 0.0003085 $\frac{\text{cm}^3}{\text{g}}$ respectively.

The mesopores and macropores analysis provides details about surface area in terms of the Brunauer-Emmett-Teller (BET) surface area (Brunauer et al., 1938) was computed by Eqn. (3.3), pore volume and pore size computes by the Horvat & Kavazoe desorption method (Horvat & Kavazoe, 1951). The estimations of these parameters are listed in Table 4.3 for all catalyst prepares in this study. The results of each parameter confirm that no discernible effect for lanthanum addition to the unpromoted bimetallic catalyst. Also, the similarity between the distribution of average Horvat & Kavazoe desorption pore size for the unpromoted and 3La promoted distributions depicted in Figure 4.5a and Figure 4.5b, also confirm the absence of a La addition effect. This may be attributed to the small quantity of La addition by comparison with the 10 wt.% nickel.

Table 4.3: N_2 – physisorption at 77 K result.

La loading on La – Ni/Al_2O_3 (Weight %)	**BET surface area, SA (m^2g^{-1})**	**Horvat & Kavazoe desorption pore size, (nm)**
0	117.115	1.1656
3	116.8445	1.1931

However, the results indicate clearly that most of desorption occurs mesoporous materials are recognized with pore diameter of 1.47 – 1.78 nm. In fact, it has been reported that mesopores adsorption and desorption implies dispersion enhancement and hence catalyst activity improvement, carbon deposition diminution and better catalyst stability (Xu et al., 2009).

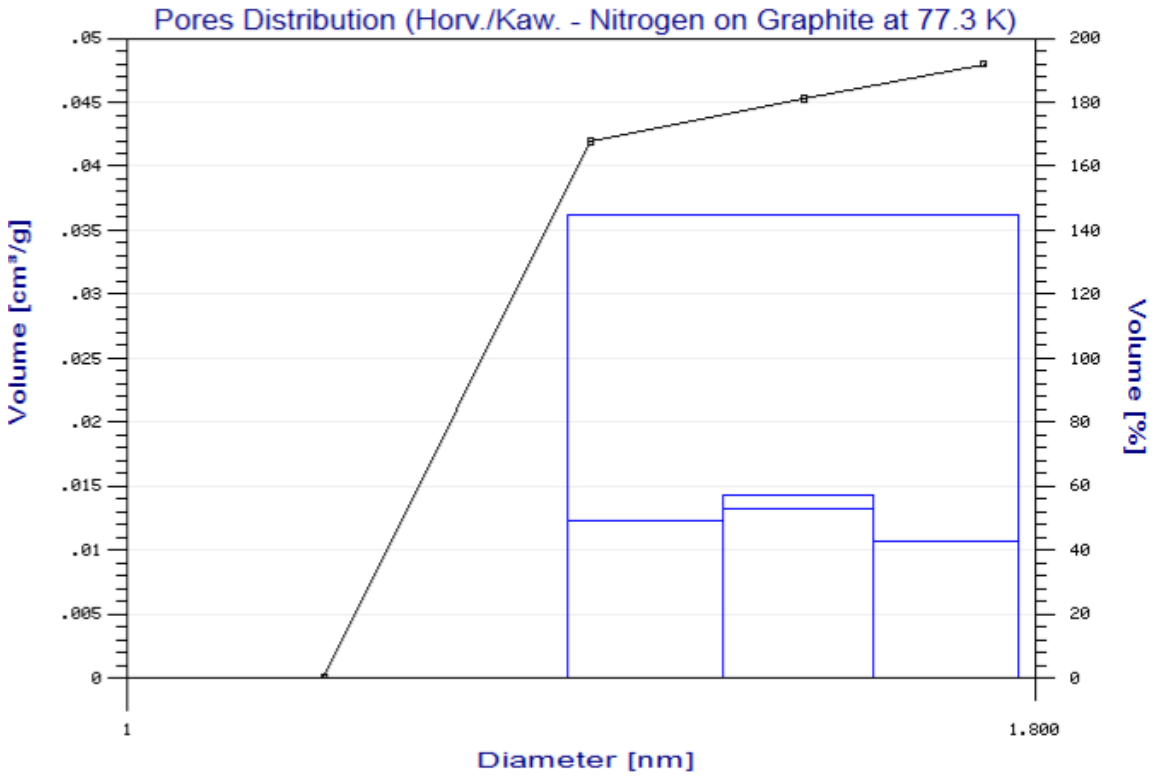

Figure 4.5a: Pore size distribution calculated using Horvat & Kavazoe desorption method for unpromoted catalyst.

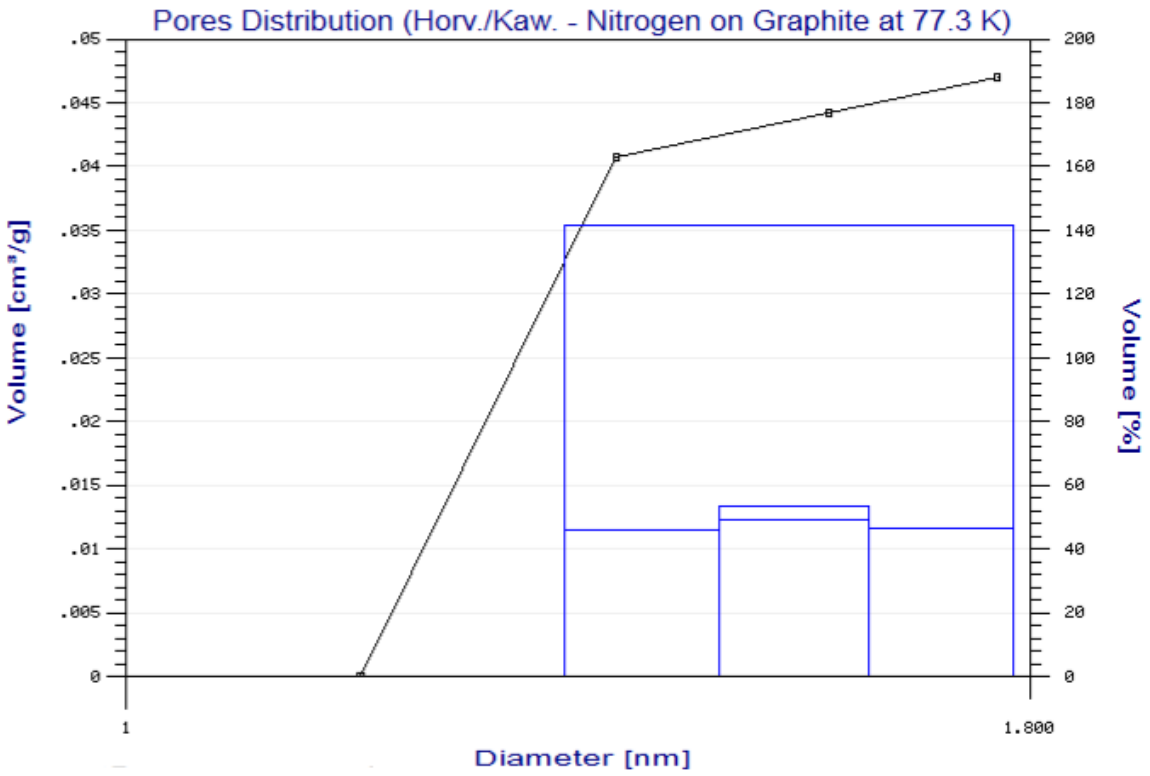

Figure 4.5b: Pore size distribution calculated using Horvat & Kavazoe desorption method for 3La promoted catalyst.

However, it is important that the BET area and average Horvat & Kavazoe desorption pore size for supported alumina, were reported as 177 m^2g^{-1}, 0.79 and 96.8 A respectively. Comparing these values with the catalyst features portrayed in Table 4.3 reveals a significant loss which may be either due to pore blockage of the support by relatively large metallic crystals. In Hardiman's study, the surface area and pore volume dropped from 181 m^2 g^{-1} and 0.81 cc g^{-1} for calcined alumina to 109 m^2 g^{-1} and 0.44 cc g^{-1} for a catalyst.

4.2.4 X-Ray Diffraction (XRD) Analysis

X-ray diffraction (XRD) was used to identify major crystalline phases and bulk-phase in the Ni/Al_2O_3 catalyst. Diffractograms of the Ni/Al_2O_3 catalyst, as well as the respective support, are displayed in Figure 4.6. Thus, XRD measurements were conducted for calcined unpromoted catalyst. As may be seen in Figure 4.6, the unpromoted catalyst were calcined at 1073 K for 6 h, the diffraction peaks of Al_2O_3 crystalline phases can be observed and was identified exist in the calcined Ni/Al_2O_3 catalyst. The peaks at the diffraction angle around 37.91^o, 46.71^o and 60.43^o were the peaks of Al_2O_3 phase (Chen et. al., 2001; Matsumura & Nakamori, 2004). However, no bulk nickel peaks appear in XRD pattern of Ni/Al_2O_3 catalyst showed in Figure 4.5. This means that there was a higher dipersion of metallic nickel in Ni/Al_2O_3 catalyst.

The nickel aluminate ($NiAl_2O_4$, spinel) phase might also be formed in this catalyst by the reaction of the Al_2O_3 with NiO as follows: $Al_2O_3 + NiO \rightarrow NiAl_2O_4$. The peaks at the diffraction angle 31.46^o, 37.13^o, 45.46^o, 60.06^o and 66.11^o were the peaks of the $NiAl_2O_4$phase exhibited strong intensities and are known as harder due to the strong interaction with the support. Besides that, the formation of the spinel phase in the Ni-based catalyst is related to the calcination temperature of the catalyst. The higher the calcinations temperature, the larger the fraction of Ni^{2+} ions converted into spinel. This conversion was practically complete for a calcination temperature of 1023 K (Rynkowski, et. al., 1993). Because the calcination

temperature of the catalysts in this study was 1073 K, the larger of amount of the spinel formed in Ni/Al_2O_3 catalyst.

The $10\%Ni/Al_2O_3$ catalyst presented also the formation of nickel oxide (NiO). The peaks at the diffraction angle 32.68^o and 66.87^o were the peaks of the NiO phase. The peak intensities of the NiO were weaker in the $10\%Ni/Al_2O_3$. This might be due to the fact that the dispersion of the NiO species became more homogeneous and higher due to nickel as precursor metal (Yang et. al., 2010). According to Li and Chen (1995), at nickel loading below 12% nickel species interact with tetrahedrally coordinated site of Al_2O_3, while at nickel loading above 12% the alumina is satured with nickel and bulk NiO is formed on the Al_2O_3 surface. NiO particles in high NiO contents tend to aggregate just as bulk due to the weak interaction with alumina (Mori et al., 2003). However, according to Li et al. (2005) mentioned with higher calcination temperatures, the crystallinity of NiO particles increases. Through this study, the calcination temperature of the catalyst was 1073 K; the amounts of the NiO phases were limited in Ni-based catalyst because NiO phases reacted with Al_2O_3 to formed $NiAl_2O_4$ at 1073 K.

From the XRD analysis, it found that the major crystalline unpromoted catalysts formed are spinel ($NiAl_2O_4$) because it is formed by the reaction of Al_2O_3 with NiO at the higher calcination temperature of the catalyst.

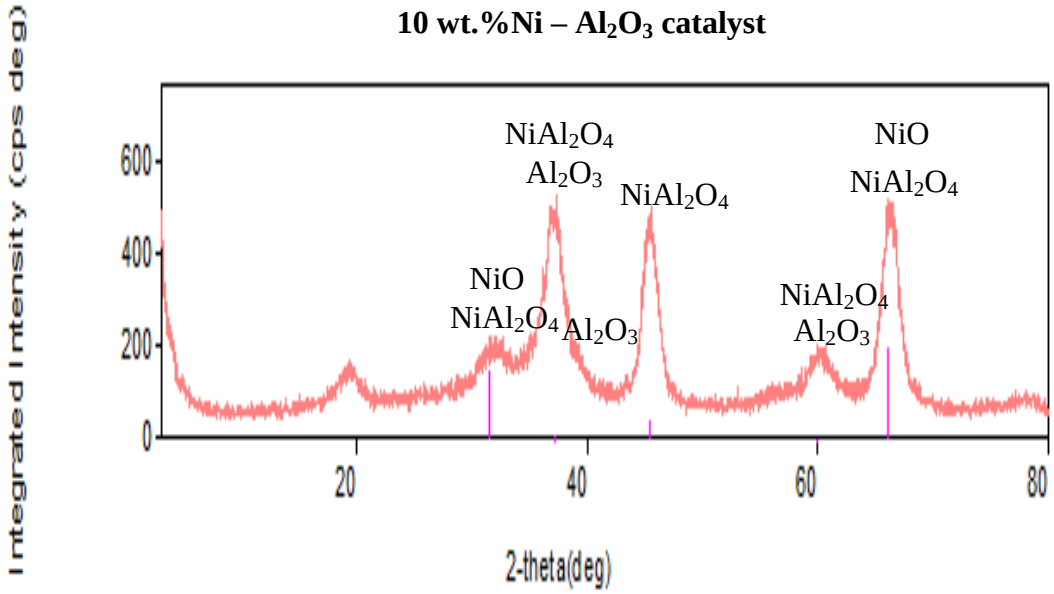

Figure 4.6: XRD pattern of the calcined 10 wt.%Ni – Al_2O_3 catalyst at 1073 K for 6 h.

CHAPTER V

CONCLUSION AND RECOMMENDATION

5.1 Conclusions

The synthesis of unpromoted (10Ni/Al_2O_3) and 3La promoted catalyst (3La-10Ni/Al_2O_3) was successfully carried out using wet co-impregnation method. The effect of lanthanum addition with 3 wt.% to the Ni/Al_2O_3 catalyst was investigated by various techniques. XRF analysis for the main metals presented in the calcined catalyst indicated a good agreement with the intended formula.

The physical attributes for unpromoted and 3La promoted catalyst showed a *Type IV* isotherm, in an indication typical of capillary condensation in mesoporous with high energy of adsorption and a hysteresis loop of *Type H1* under new

classification system revealing cylindrical pore geometry or spheroidal particles with reasonably uniform size.

This negative effect for the addition of La to the unpromoted catalyst was confirmed by the similar detailed results of BET area and Horvat & Kavazoe desorption pore size for all freshly calcined catalysts. However, the addition of La to the Ni-based catalyst did not imply a significant change in the chemisorptive properties.

The morphological features of the unpromoted catalyst were examined by XRD. In XRD pattern analysis, diffraction angle around 37.91^{o}, 46.71^{o} and 60.43^{o} were linked Al_2O_3. However, no bulk nickel peaks appear in XRD pattern, while a weak NiO presented in Ni/Al2O3 catalyst. Besides that, the major crystalline unpromoted catalysts formed are spinel ($NiAl_2O_4$) because it is formed by the reaction of Al_2O_3 with NiO at the higher calcination temperature of the catalyst.

5.2 Recommendations

Based on the outcomes of this research and some of the ideas reported in the literature, the following remarks can be considered for future work:

- Catalyst preparation stages should be investigated thoroughly based on the surface chemistry.

- The effect of manual stirring during the first twelve hours of the drying process upon impregnation on the dispersion and other features need to be examined.
- The influence of the pH level during preparation methods may need to be verified under the advance control instrument.
- Higher hydrocarbons are known to require activation energy; hence, the metal loading of Ni is advised to be verified.
- Other basis promotes need to be examined to find the best additive that gives the highest syngas production and carbon resistance along with cheapest price.

REFERENCES

Ahmed, S., & Krumpelt, M. (2001). Hydrogen from hydrocarbon fuels for fuel cells. *International journal of hydrogen energy, 26*, 291-301.

Aligizaki, K.K. (2006). Pore structure of cement-based materials: Testing, interpretation and requirements. *Taylor & Francis.*

Armor, J. N. (1999). The multiple roles for catalysis in the production of H_2. *Applied catalysis A: General, 179,* 159-176.

Armor, J. N. (2005). Catalysis and the hydrogen economy. *Catalysis letters, 101(3 – 4),* 131 – 135.

Ayabe, S., Omoto, H., Utaka T., Kikuchi, R., Sasaki, K., Teraoka, Y., & Eguchi, K. (2003). Catalytic autothermal reforming of methane and propane over supported metal catalysts. *Applied Catalysis A: General, 241,* 261 – 269.

Bartholomew, C. H. (2001). Mechanisms of catalyst deactivation. *Applied catalysis A: General, 212(1 – 2), 17 – 60.*

Bermúdez, J. M., Arenillas, A., & Menéndez, J. A. (2011). Syngas from CO_2 reforming of coke oven gas: Synergetic effect of activated carbon/Ni/γ-Al_2O_3 catalyst. *International journal of hydrogen energy, 36,* 13361-13368.

Bitter, J. H., Seshan, K., & Lercher, J. A. (1997). The state of zirconia supported platinum catalysts for CO_2/CH_4 reforming. *Journal of catalyst, 171,* 279 – 286.

Bradford, M. C. J., & Vannice, M. A. (1999). The role of metal support interactions in CO_2 reforming of CH_4. *Catalysis today, 50,* 87 – 96.

Bradford, M. C. J., & Vannice, M. A. (1996). Catalytic reforming of methane with carbon dioxide over nickel catalysts II. Reaction kinetics. *Applied catalysis A: General, 142,* 97-122.

Bradford, M. C. J., & Vannice, M. A. (1996). Catalytic reforming of methane with carbon dioxide over nickel catalysts I. Catalyst characterization and activity. *Applied catalysis A: General, 142,* 73 – 96.

Brunauer, S., Emmett, P., & Teller, E. (1938). Adsorption of gases in multimolecular layers. *Journal of the American chemical society, 60(2), 309 – 319.*

Brunauer, S., Deming, L. S., Deming, W. E., & Teller, E. (1940). On a theory of the van der waals adsorption of gases. *Journal of the American chemical society, 62(7), 1723 – 1732.*

Cheng, T. S., Rodriguez, N. M., & Baker, R. T. K. (1996). Carbon deposition on supported nickel particles. *Journal of catalysis, 123,* 486 – 495.

Cheng, Z. X., Zhao, X. G.., Li, J. L., & Zhu, Q. M. (2001). Role of support in CO_2 reforming of CH_4 over a Ni/γ-Al_2O_3 catalyst. *Applied catalysis A: General, 205,* 31 - 36.

Choudhary, V. R.., Rane, V. H., & Rajput, A. M. (1996). Beneficial effects of cobalt addition to Ni-catalysts for oxidation conversion of methane to syngas. *Applied catalysis A: General, 162,* 235 – 238.

Choudhary, V. R., Uphade, B. S., & Mamman, A. S. (1997). Oxidative conversion of methane to syngas over nickel supported on commercial low surface area porous catalyst carriers precoated with alkaline and rare earth oxides. *Journal of catalysis, 172,* 281-293.

Condon, J. (2006). Surface area and porosity determinations by physisorption: Measurements and theory.*Amsterdam: Elsevier Science Ltd.*

Daza, C. E., Gallego, J., Mondragón, F., Moreno, S., & Molina, R. (2010). High stability of Ce-promoted Ni/Mg-Al catalysts derived from hydrotalcites in dry reforming of methane. *Fuel, 89,* 592 – 603.

De Boer, J. (1958). The structure and properties of porous materials. *London: Butterworths, 405.*Ding, R. G., Yan, Z. F., Song, L. H., & Liu, X. M. (2001). Journal natural gas chemistry, 10, 273 – 230.

Dong, W. S., Roh, H. S., Jun, K. I., Park, S. E., & Oh, Y. S. (2002). Methane reforming over Ni/Ce-ZrO_2 catalyst: Effect of nickel content. *Applied catalysis A: General, 226,* 63 – 72.

Edwards, J. H., Do, K. T., & Maitra, M. (1996). The use of solar-based CO_2/CH_4 reforming for reducing greenhouse gas emissions during the generation of electricity and process heat. *Energy conversions management, 37(6 – 8),* 1339 – 1344.

Eltejaei, H., Bozorgzadeh, H. R., Towfighi, J., Omidkhah, M. R., Rezaei, M., Zanganeh, R., Zamaniyah, A., & Ghalam, A. Z. (2012). Methane dry reforming on $Ni/Ce_{0.75}Zr_{0.25}O_2 - MgAl_2O_4$ and $Ni/Ce_{0.75}Zr_{0.25}O_2 - \gamma$-alumina: Effects of support composition and water addition. *International journal of hydrogen energy, 37,* 4107-4118.

Engler, B., Koberstein, D., Lindner, D., & Lox, E. (1991). The influence of three-way catalyst parameters on secondary emission. Catalysis and automotive pollution control II, 249, 641 – 655.

Fathi, M., Bjorgum, E., Viig, T., & Rokstad, O. A. (2000). Partial oxidation of methane to synthesis gas: Elimination of gas phase oxygen. *Catalysis today, 63,* 489 – 497.

Fidalgo, B., Zubizarrets, L., Berm*ú*dez, J. M., Arenillas, A., & Men*é*ndez, J. A. (2010). Synthesis of carbon-supported nickel catalysts for the dry reforming of CH_4. *Fuel processing technology, 91,* 765 – 769.

Forzatti, P., & Lietti, L. (1999). Catalyst deactivation. *Catalysis today, 52(2 – 3), 165 – 181.*

Gadalla, A. M., & Bower, B. (1988). The role of catalyst support on the activity of nickel for reforming methane with CO_2. *Chemical engineering science, 43,* 3049 – 3053.

Gallego, G. S., Mondragón, F., Tatibouët, J., Barrault, J., & Batiot-Dupeyrat, C. (2008). Carbon dioxide reforming of methane over La_2NiO_4 as catalyst precursor – characterization of carbon deposition. *Catalysis today, 133 – 135,* 200 – 209.

Guo, J. J., Lou, H., & Zheng., X. M. (2007). Carbon, 45, 1314 – 1334.

Gregg, S. J. & Sing, K. S. W. (1982). Adsorption, surface area and porosity. *2 ed., London: Academic Press.*

Hardiman, K.M. (2007). Propane reforming under carbon-induced deactivation: Catalyst design and reactor operation.*The University of New South Wales: Sydney.*

Horiuchi, T., Sakuma, K., Fukui, T., Kubo, Y., Osaki, T., & Mori, T. (1996). Suppression of carbon deposition in the CO_2-reforming of CH_4 by adding basic metal oxides to a Ni/Al_2O_3 catalyst. *Applied catalysis A: General, 144,* 111-120.

Horvat, E.P., & Kavazoe, P. P. (1951). The determination of pore volume and area distributions in porous substances. I. Computations from nitrogen isotherms. *Journal of the American chemical society,73(1), 373 – 380.*

Hou, Z., Yokota, O., Tanaka, T., & Yashima, T. (2003). Characterization of Ca-promoted Ni/α-Al_2O_3 catalyst for CH_4 reforming with CO_2. *Applied catalysis A: General, 253,* 381 – 387.

Jungke, X., Wei, Z., Jihui, W., Zhaojing, L., & Jianxin, M. (2009). Characterization and analysis of carbon deposited during the dry reforming of methane over $Ni/La_2O_3/Al_2O_3$ catalysts. *Chinese journal of catalysis, 30(11),* 1076 – 1084.

Kim, J., Suh, D. J., Park, T., & Kim, K. (2000). Effect of metal particle size on coking during CO_2 reforming of CH_4 over Ni-alumina aerogel catalysts. *Applied catalysis A: General, 197,* 191 – 200.

Kusakabe, K., Sotowa, K. I., Eda, T., & Iwamoto, Y. (2004). Methane steam reforming over Ce-ZrO_2-supported noble metal catalysts at low temperature. *Fuels processing technology, 86,* 319 – 326.

Laosiripojana, N., Chadwick, D., & Assabumrungrat, S. (2008). Effect of high surface area CeO_2 and Ce-Zr_2O supports over Ni catalyst on CH_4 reforming with H_2O in the presence of O_2, H_2, and CO_2. *Chemical engineering journal, 138,* 264-273.

Li, B., Watanable, R., Maruyama, K., Nurunnabi, M., Kunimori, K., & Tomishige, K. (2005). High combustion activity of methane induced by reforming gas over Ni/Al_2O_3 catalysts. *Applied catalysis A: General, 290,* 36 – 45.

Li, C., & Chen, Y. W. (1995). Temperature-programmed reduction studies of nickel oxide/alumina catalysts: Effects of the preparation method. *Thermochimica acta, 256, 457.*

Liguras, D. K., Kondarides, D. I., & Verykios, X. E. (2003). Production of hydrogen for fuel cells by steam reforming of ethanol over supported noble metal catalysts. *Applied catalysis B: Environmental, 43,* 345 – 354.

Lobeng, L. S., Su, L., Wang, H., Shen, W., Bao, X., & Xu, Y. (1997). Rare-earth oxides promoted nickel based catalyst for methane dry reforming. *Journal of catalysis, 29,* 97 – 115.

Lowell, S. (2004). Characterization of porous solids and powders: Surface area, pore size, and density. *Kluwer Academic Publishers.*

Lu, M., Praharso, & Trimm, D. L. (1999). Rare-earth oxides promoted nickel based catalyst for steam reforming. *Materials science forum, 315 – 317,* 187 – 193.

Matsumura, Y., & Nakamori, T. (2004). Steam reforming of methane over nickel catalyst at low reaction temperature. *Applied catalysis A: General, 258,* 107 – 114.

Mori, H., Wen, C., Otomo, J., Eguchi, K., Takahashi, H. (2003). Investigation of the interaction between NiO and Yttria-stabilized zirconia (YSZ) in the NiO/YSZ composite by temperature-programmed reduction technique. *Applied catalysis A: General, 245, 79.*

Morterra, A. C., Engelhard, P. A., & Weisang, J. E. (1996). Surface study of platinum-tin bimetallic reforming catalysts. *Journal of Catalysis, 56,* 65 – 72.

Murata, K., Wang, L., Saito, M., Inaba, M., Takahara, I., & Mimura, N. (2004). Hydrogen production form steam reforming of hydrocarbons over alkaline-earth metal modified Fe- or Ni-based catalysts. *Energy and fuels, 18,* 122 – 126.

Nakagawa, K., Nishimoto, H., Kikuchi, M., Egashira, S., Enoki, Y., Ikenaga, N., Suzuki, T., Nishitani-Gamo, M., Kobayashi, T., & Ando, T. (2003). Synthesis gas production from methane using oxidized-diamond-supported group VIII metal catalysts. *Energy and fuels, 17,* 971 – 976.

Olsbye, U., Salgtern, Å., Blom, R., Dahl, I. M., & Fjellvåg, H. (1997). Characterization of Ni on La modified Al_2O_3 catalysts during CO_2 reforming of methane. *Applied catalysis A: General, 165,* 379 – 390.

Özkara-Aydlnoğlu, S., Özensoy, E., & Aksoylu, A. E. (2009). The effect of impregnation strategy on methane dry reforming activity of Ce promoted Pt/ZrO_2. *International journal of hydrogen energy, 169,* 1 – 12.

Özkara-Aydlnoğlu, S., & Aksoylu, A. E. (2011). CO_2 reforming of methane over Pt-Ni/Al_2O_3 catalysts: Effects of catalyst composition, and water oxygen addition to the feed. *International journal of hydrogen energy, 36,* 2950 – 2959.

Palm, C., Cremer, P., Peters, R., & Stolten, D. (2002). Small-scale testing of a precious metal catalyst in the autothermal reforming of various hydrocarbons feeds. *Journal of power sources, 106,* 231 – 237.

Peña, M. A., Gómez, J. P., & Fierro, J. L. G. (1996). New catalytic routes for syngas and hydrogen production. *Applied catalysis A: General, 144,* 7 – 57.

Qin, D., & Lapszewics, J. (1994). Study of mixed steam and CO_2 reforming of CH_4 to syngas on MgO-supported metals. *Catalysis today, 21(2 – 3),* 551 – 560.

Reshetenko, T. V., Avdeeva, L. B., Khassin, A. A., Kustova, G. N., Ushakov, V. A., Moroz, E. M., Shmakov, A. N., Kriventsov, V. V., Kochubey, D. I., Pavlyukhin, Yu. T., Chuvilin, A. L., & ismagilov, Z. R. (2004). Co-precipitated iron-containing catalysts ($Fe-Al_2O_3$, $Fe-Co-Al_2O_3$, $Fe-Ni-Al_2O_3$) for methane

decomposition at moderate temperatures I. Genesis of calcined and reduced catalysts. *Applied catalysis A: General, 268,* 127 – 138.

Richardson, J. T., & Paripatyadar, S. A. (1990). Carbon dioxide reforming of methane with supported rhodium. *Applied catalysis, 61(1),* 293 – 309.

Rostrup-Nielsen, J. R. (1984). Catalytic steam reforming. In, *Catalysis, science and technology* (Anderson, J. R., & Boudart, M., eds.), Springer Verlag, Berlin, chapter 1, 5, 1 – 117.

Rostrup-Nielsen, J. R. (1975). Activity of nickel catalysts for steam reforming of hydrocarbons. *Journal of catalysis, 31,* 173 – 199.

Rynkowski, J. M., Paryjczak, T., & Lenik, M. (1993). On the nature of oxidic phases in $NiO/\gamma\text{-}Al_2O_3$ catalysts. *Applied catalysis A: General, 106, 73.*

Sing, K. S. W. (1982). Adsorption, surface area and porosity. *2 ed., London: Academic Press.*

Soria, J. H. Goguet, A., Meunier, F. C., Breen, J. P., & Burch, R. (1996). Catalysis by alloys and bimetallic clusters. *Accounts of chemical research, 20,* 15 – 20.

Souza, M. M. V. M., Clav*ý*, L., Dubois, V., Perez, C. A. C., & Schmal, M. (2004). Activation of supported nickel catalysts for carbon dioxide reforming of methane. *Applied catalysis A: General, 272,* 133 – 139.

Takeguchi K. H. (2003). Titania-supported cobalt and nickel bimetallic catalysts for carbon dioxide reforming of methane. *Journal of catalysis, 232,* 268 – 275.

Tsang, S. C., Claridge, J. B., & Green, M. L. H. (1995). Recent advances in the conversion of methane to synthesis gas. *Catalysis today, 23,* 3 – 15.

Tsipouriari, V. A., Efstathiou, A. M., Zhang, Z. L., & Verykios, X. E. (1994). Reforming of methane with carbon dioxide to synthesis gas over supported Rh catalysts. *Catalysis today, 21(2-3),* 579-587.

Wan, H., Li, X., Huang, B., Wang, K., & Li, C. (2007). Effect of Ni loading and $Ce_xZr_{1-x}O_2$ promoter on Ni-based SBA-15 catalyst for steam reforming of methane. *Journal of natural gas chemistry, 16,* 139-147.

Wang, S., & Lu, G. Q. M. (1998). Role of CeO_2 in Ni/CeO_2-Al_2O_3 catalysts for carbon dioxide reforming of methane. *Applied catalysis B: Environmental, 19,* 267 – 277.

Wang, S., & Lu, G. Q. M. (2001). CO_2 reforming of methane on Ni catalysts: Effects of the support phase and preparation technique. *Applied catalysis B: Environmental, 16,* 269 – 277.

Wang, H., Li, Z., & Tian, S. (2004). Effect of promoters on the catalytic performance of Ni/Al_2O_3 catalyst for partial oxidation of methane to syngas. *Reaction kinetic catalyst letters, 83(2),* 245 – 252.

Wilhelm, D. J., Simbeck, D. R., Karp, A. D., & Dickenson, R. L. (2001). Syngas production for gas-to-liquids applications: Technologies, issues and outlook. *Fuel processing technology, 71(1 – 3), 139 – 148.*

Williams, M. (2002). National energy technology laboratory/strategic center for natural gas 'Secretary's Weekly Report'. *International journal of hydrogen energy, 19,* 184 – 244.

Xu, Z., Li, Y., Zhang, J., Chang, L., Zhou, R., & Duan, Z. (2001). Bound-state Ni-based catalyst for CH_4/CO_2 reforming. *Applied catalysis A: General, 210,* 45 – 53.

Xu, J., Zhou, J., Wang, J., Li, Z., & Ma, J. (2009). Characterization and analysis of carbon deposited during the dry reforming of methane over $Ni/La_2O_3/Al_2O_3$ catalysts. *Chinese journal of catalyst, 30(11),* 1076 – 1084.

Yang, R., Xing, C., Lv., C., Shi, L., & Tsubaki, N. (2010). Promotional effect of La2O3 and CeO2 on Ni/γ- Al_2O_3 catalysts for CO_2 reforming of CH_4. *Applied catalysis A: General, 385,* 92-100.

Zhang, Z., & Verykios X. E. (1996). Carbon dioxide reforming of methane to synthesis gas over Ni/La_2O_3 catalysts. *Applied catalysis A: General, 138,* 109 – 133.

APPENDIX A

SAMPLE CALCULATION FOR PREPARATION OF STOCK SOLUTION DURING CATALYST PREPARATION

APPENDIX A

SAMPLE CALCULATION FOR PREPARATION OF STOCK SOLUTION DURING CATALYST PREPARATION.

Catalyst type : $10Ni - 90Al_2O_3$

Metal salt used : $Ni(NO_3)_2.6H_2O$

Molecular Weight $Ni(NO_3)_2.6H_2O$:290.79 g mol^{-1}

Pore Volume of Al_2O_3 : 0.8 ml g^{-1}

Basis : 100 g Al_2O_3

Thus,

Weight of $Ni(NO_3)_2.6H_2O$ salt required $= 50\ \text{g} \times \frac{10}{90} \times \frac{290.79\ \text{g mol}^{-1}}{58.71\ \text{g mol}^{-1}} = 27.5166\ \text{g}$

Volume of water added $= 2 \times 0.8\ \text{ml g}^{-1} \times 50\ \text{g} = 80\ \text{ml}$

Catalyst type : $3La - 10Ni - 87Al_2O_3$

Metal salt used : $Ni(NO_3)_2.6H_2O$

Promoter metal used : $La(NO_3)_3$

Molecular Weight of $Ni(NO_3)_2.6H_2O$:290.79 g mol^{-1}

Molecular Weight of $La(NO_3)_3$: 325. 81 g mol^{-1}

Pore Volume of Al_2O_3 : 0.8 ml g^{-1}

Basis : 50 g Al_2O_3

Thus,

Weight of $Ni(NO_3)_2.6H_2O$ salt required $= 50\text{ g} \times \frac{10}{87} \times \frac{290.79\text{ g mol}^{-1}}{58.71\text{ g mol}^{-1}} = 28.4655\text{ g}$

Weight of $La(NO_3)_3$ required $= 50\text{ g} \times \frac{3}{87} \times \frac{325.81\text{ g mol}^{-1}}{138.91\text{ g mol}^{-1}} = 4.0439\text{ g}$

Volume of water added $= 2 \times 0.8\text{ ml g}^{-1} \times 50\text{ g} = 80\text{ ml}$

The calculated amounts of salts and promoter metal added in the preparation of catalyst employed are summarized in Table A1. Further, Table A2 shows amount of water added during impregnation of catalysts.

Table A1 Amount of salts and promoter metal added in catalysts.

Catalyst	**Amount of Salts and Promoter Added (g)**	
	$Ni(NO_3)_2.6H_2O$	**$La(NO_3)_3$**
$10Ni - 90Al_2O_3$	27.5166	-
$3La - 10Ni - 87Al_2O_3$	28.4655	4.0439

Table A2: Amount of water added during impregnation of catalyst.

Catalyst	**Amount of Water Added (ml)**
$10Ni - 90Al_2O_3$	80
$3La - 10Ni - 87Al_2O_3$	80

APPENDIX B

METHODOLOGY

APPENDIX B-1

PREPARATION OF UNPROMOTED CATALYST

Figure B-1.1: Al_2O_3 support catalyst

Figure B-1.2: $Ni(NO_3)_2.6H_2O$ salts.

Figure B-1.3: Wet co-impregnation was carried out at room temperature for 3hr.

Figure B-1.4: The slurry was dried at 120 ^{o}C for 12 hr.

Figure B-1.5: The dried solid was calcined at 800 ^{o}C for 6 hr.

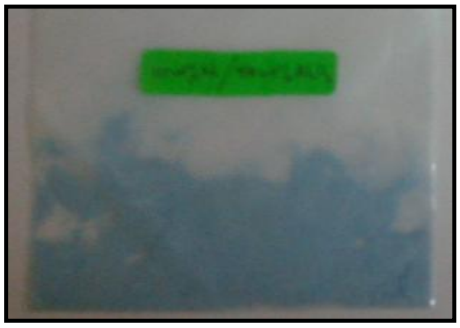

Figure B-1.6: 10Ni–90Al_2O_3 catalyst.

APPENDIX B-2

PREPARATION OF 3La PROMOTED CATALYST

Figure B-2.1: Al_2O_3 support catalyst.

Figure B-2.2: $Ni(NO_3)_2.6H_2O$ salts.

Figure B-2.3: First wet co-impregnation was carried out at room temperature for 3hr.

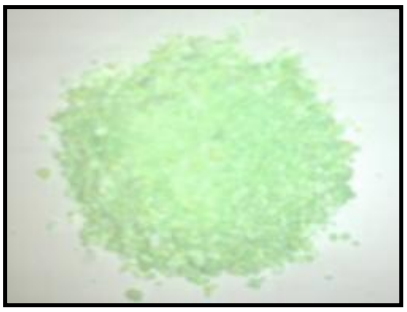

Figure B-2.4: Dried solid after first wet co-impregnation.

Figure B-2.5: $La(NO_3)_3$ metal

Figure B-2.6: Second wet co-impregnation was carried out at room temperature for 3hr.

Figure B-2.7: The slurry was dried at 120 ^{o}C for 12 hr.

Figure B-2.8: The dried solid was calcined at 800 ^{o}C for 6 hr.

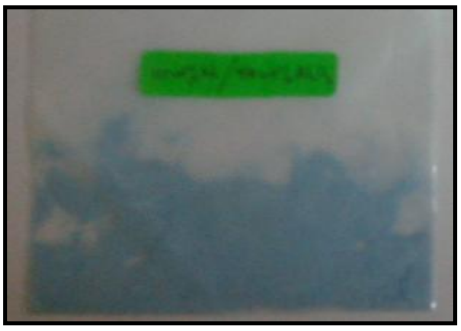

Figure B-2.9: 3La–10Ni–90Al_2O_3 catalyst.

APPENDIX C

RESULT & DISCUSSION

APPENDIX C-1

X-RAY FLUORESCENSE (XRF) RESULTS

CENLAB/F/007

Universiti Malaysia PAHANG

CENTRAL LABORATORY
Universiti Malaysia Pahang, Lebuhraya Tun Razak,
26300 Kuantan, Pahang Darul Makmur.
Tel: 09-5493344/8097 Fax: 09-5493353
E-mail: ucl@ump.edu.my

CERTIFICATE OF ANALYSIS (COA)

To :	Norzaini bin Abd Rahim	Attn :	
Address :	FKKSA, UMP		
c.c. :		Page :	2 pages
Fax No :	Tel No : 013-4467216		Sample Lab No: 2013/010

Sample description : Two samples in powdered form

Sample marking : Catalyst

Date of sample received : 26/12/2012

Date reported : 04/01/2013

RESULTS:

Sample 1: Unpromoted Catalyst

No	Parameter	Result	Unit	Test Method
1.	Aluminium (Al)	50.64	%	Quantexpress (Best Detection)
2.	Nickel (Ni)	9.5	%	Quantexpress (Best Detection
3.	Chlorine (Cl)	0.03	%	Quantexpress (Best Detection
4.	Iron (Fe)	0.01	%	Quantexpress (Best Detection
5.	Sulphur (S)	89	ppm	Quantexpress (Best Detection

Figure C-1.1: XRF analysis for unpromoted catalyst

Sample 2: 3La promoted Catalyst

No	Parameter	Result	Unit	Test Method
1.	Aluminium (Al)	50.37	%	Quantexpress (Best Detection)
2.	Nickel (Ni)	9.3	%	Quantexpress (Best Detection
3.	Lanthanum (La)	2.5	%	Quantexpress (Best Detection
4.	Sulphur (S)	0.84	%	Quantexpress (Best Detection
5.	Iron (Fe)	0.01	ppm	Quantexpress (Best Detection

The certificate shall not be reproduced except in full without the written approval of the laboratory.

The above analysis is based on the sample submitted by the customer.

SYAHIDAH BINTI ALWI
PEGAWAI SAINS
MAKMAL BERPUSAT
JABATAN PENYELIDIKAN & INOVASI
UNIVERSITI MALAYSIA PAHANG
LEBUHRAYA TUN RAZAK
26300 GAMBANG KUANTAN, PAHANG

Figure C-1.2: XRF analysis for 3La promoted catalyst

APPENDIX C-2

FTIR ANALYSIS

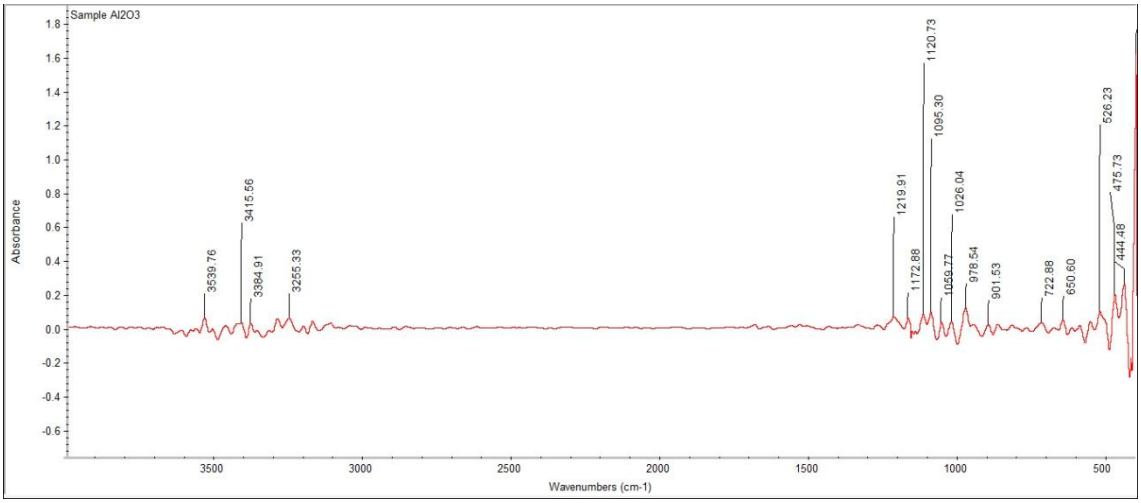

Figure C-2.1: FTIR analysis for alumina support catalyst.

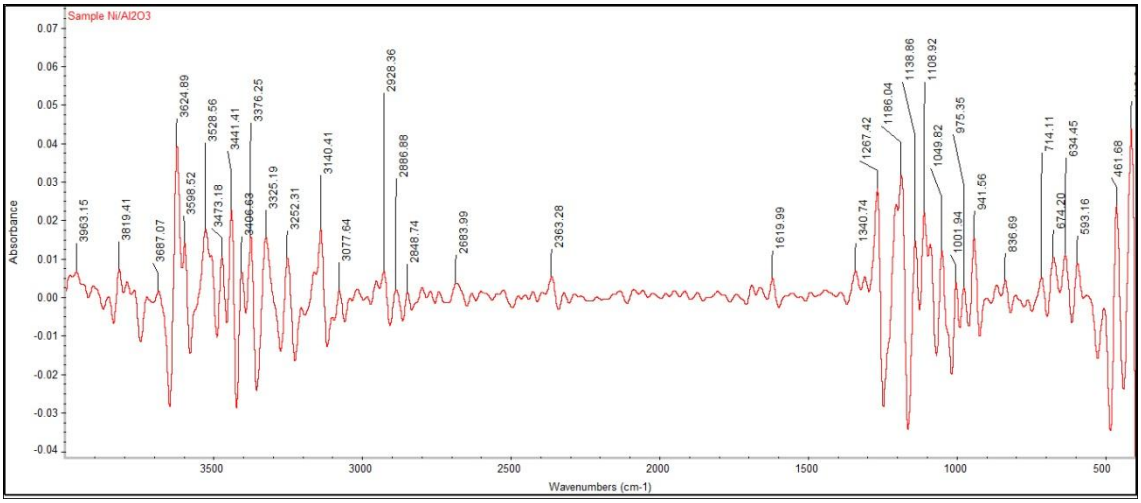

Figure C-2.2: FTIR analysis for Ni/Al_2O_3 catalyst.

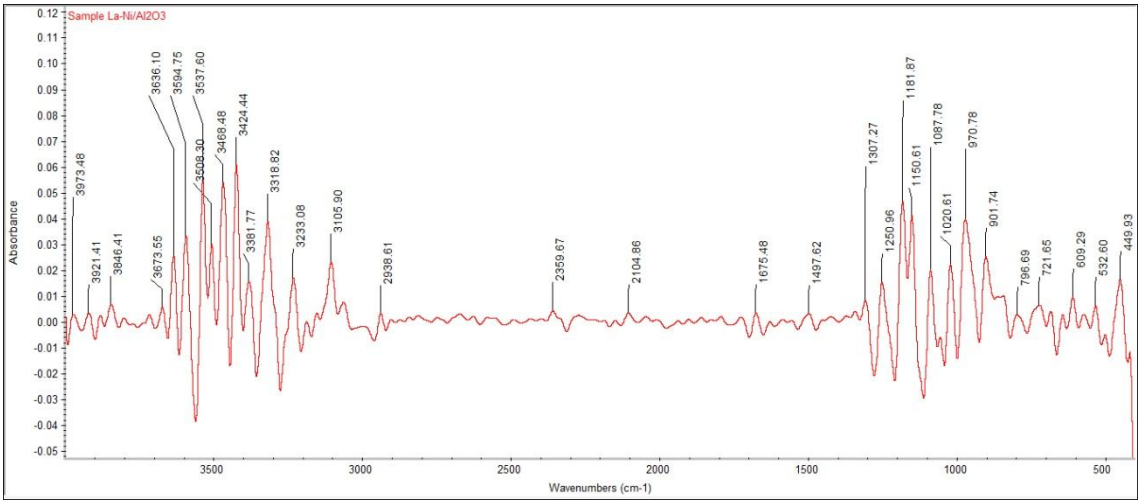

Figure C-2.3: FTIR analysis for La- Ni/Al_2O_3 catalyst.

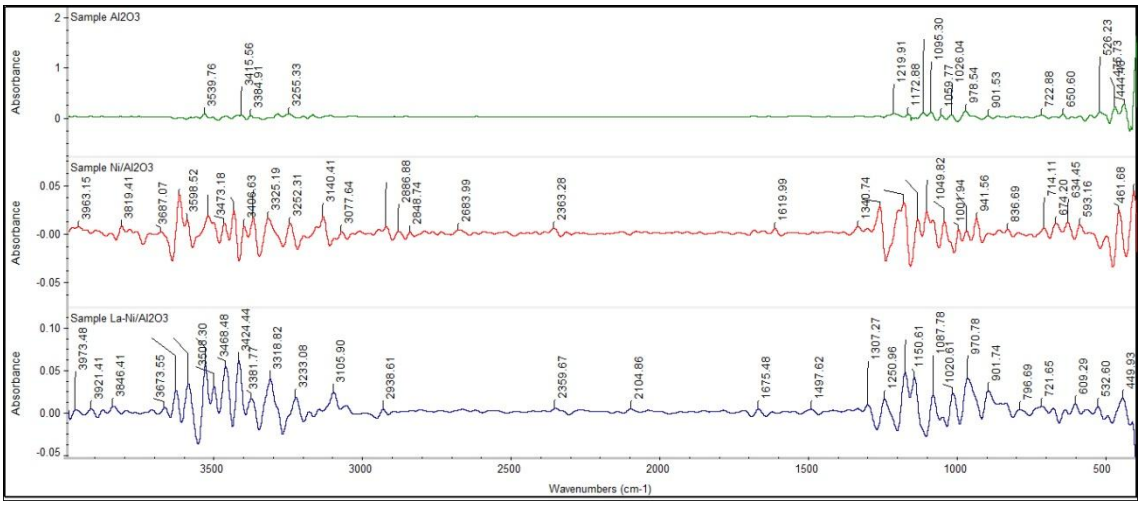

Figure C-2.4: FTIR analysis for comparison of alumina, Ni/Al_2O_3, and La- Ni/Al_2O_3 catalyst.

APPENDIX C-3

BET ANALYSIS

La-Ni/Al2O3 METHOD FOR UKNOWN
Test Report

Report date:7/12/2012

ANALYSIS INFORMATION

Sample Info.
File Name: C:\Surfer\result\Zaini KA10149\La-Ni-AL2O3 METHOD UKNOWN SURFACE061212 - with blank.srf
Sample Name: La-Ni/Al2O3 METHOD FOR UKNOWN SURFACE AREA
Preparation: 300°C overnight
Company: thermo
Date: 6/12/2012
Date of Start Analysis: 6/12/2012 11:50:29 AM
Date of End Adsorption: 6/12/2012 6:10:41 PM
Date of End Desorption: 7/12/2012 1:42:52 AM
Sample mass (g): .2747
Sample density (g/cm³): 2.9996

Acquisition Parameters
Analysis Type Ads.+ Des.
Saturation method: Auto-Cal P.Sat
Starting Load. P.(torr) 500
Min. Sat. Press.(torr) 720
Max .Ads. Press.(torr): 1000
Min.Des.Press. (torr): 100
Acquisition Mode: Zone

Zone ads.	Step(torr)		Range(torr)	Delta P.(torr)	Eq.T.(s)
1	20	300	.1	90	
2	40	600	.3	90	
3	30	800	.5	90	

Zone des.	Step(torr)		Range(torr)	Delta P.(torr)	Eq.T.(s)
1	30	600	.5	90	
2	40	100	.3	90	

Blank Parameters
CA0: .086037
CA1: 1
CA2: 0
Points Range: 1 - 7
CD0: 8.608901E-02
CD1: -.1041311
CD2: 0
Filename: C:\Surfer\result\Zaini KA10149\Burette 3_Method BLANK_301112.blk

Analytical Conditions
Gas Name: N2 Nitrogen
Gas mol. weight (g/mol) : 28.01
Gas molecolar area (A²) : 16.2
Liquid gas density (g/cm³): .8086

Page 1/8

La-Ni/Al2O3 METHOD FOR UKNOWN
Test Report

Report date:7/12/2012

ANALYSIS INFORMATION

Sample Info.
File Name: C:\Surfer\result\Zaini KA10149\La-Ni-AL2O3 METHOD UKNOWN SURFACE061212 - with blank.srf
Sample Name: La-Ni/Al2O3 METHOD FOR UKNOWN SURFACE AREA
Preparation: 300°C overnight
Company: thermo
Date: 6/12/2012
Date of Start Analysis: 6/12/2012 11:50:29 AM
Date of End Adsorption: 6/12/2012 6:10:41 PM
Date of End Desorption: 7/12/2012 1:42:52 AM
Sample mass (g): .2747
Sample density (g/cm³): 2.9996

Acquisition Parameters
Analysis Type Ads.+ Des.
Saturation method: Auto-Cal P.Sat
Starting Load. P.(torr) 500
Min. Sat. Press.(torr) 720
Max .Ads. Press.(torr): 1000
Min.Des.Press. (torr): 100
Acquisition Mode: Zone

Zone ads.	Step(torr)	Range(torr)	Delta P.(torr)	Eq.T.(s)
1	20 300	.1	90	
2	40 600	.3	90	
3	30 800	.5	90	

Zone des.	Step(torr)	Range(torr)	Delta P.(torr)	Eq.T.(s)
1	30 600	.5	90	
2	40 100	.3	90	

Blank Parameters
CA0: .086037
CA1: 1
CA2: 0
Points Range: 1 - 7
CD0: 8.608901E-02
CD1: -.1041311
CD2: 0
Filename: C:\Surfer\result\Zaini KA10149\Burette 3_Method BLANK_301112.blk

Analytical Conditions
Gas Name: N2 Nitrogen
Gas mol. weight (g/mol) : 28.01
Gas molecolar area (A²) : 16.2
Liquid gas density (g/cm³): .8086

APPENDIX C-4

X-RAY DIFFRACTION (XRD) ANALYSIS

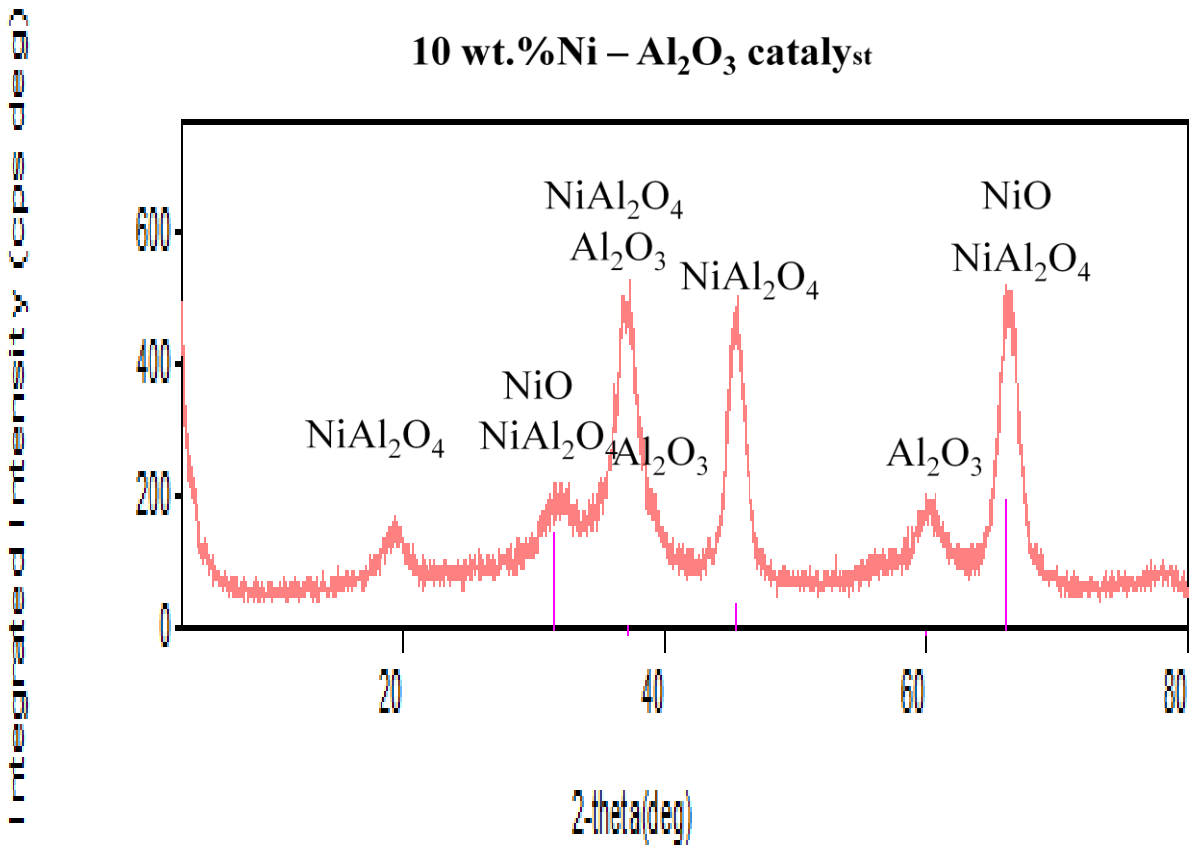

Figure C-4.1: XRD analysis for Ni/Al_2O_3 catalyst.